Validation and verification of FLUKA for neutron shielding problems

This dissertation is submitted in partial fulfilment for the degree of Masters of Engineering at the University of Cape Town.

Prepared by Mbulelo Dondolo

Supervised by Dr Tanya Hutton and Dr Tom Leadbeater, Department of Physics, UCT.

January 2021

ACKNOWLEDGEMENT

This is a Masters of Engineering dissertation at the University of Cape Town (UCT), Western Cape. I would first like to thank my supervisors, Dr Tanya Hutton, and Dr Tom Leadbeater, for everything they taught me about FLUKA and neutron transport physics. I would also like to thank the Department of Physics and the Department Electrical Engineering, for accepting me as a student and giving me the opportunity to research in this very exciting project. I would also like to express my deep gratitude to all the support I received during my studies at UCT while writing this dissertation.

Finally, I would like to thank everyone else who in some way have helped me in my studies.

DECLARATION

I know that plagiarism is wrong. Plagiarism is to use another's work and pretend that it is your own.

I have used a recognised convention for citation and referencing. Each significant contribution and quotation from the works of other people has been attributed, cited and referenced.

I certify that this submission is all my own work.

I have not allowed and will not allow anyone to copy this work with the intention of passing it off as his or her own work.

This dissertation has been submitted to the Turnitin module (or equivalent similarity and originality checking software), and I confirm that my supervisors have seen my report and any concerns revealed by such have been resolved with my supervisors.

Signature: Signed by candidate **Date: 05** April 2021

ABSTRACT

Monte Carlo-based radiation transport codes provide an opportunity to simulate situations with various levels of activation and different induced nuclides. However, to test their reliability, it is important to verify the simulation codes by comparing them with experimental data. In this study, validation of simulation models with experiments was performed with the purpose of determining the reliability of the simulation/experimental results.

Concrete is the most generally used shield material as it is inexpensive and adjustable for any construction design. Radiation shielding properties of concrete may vary depending on the concrete composites. In this thesis, the fluences (i.e. the flux integrated over time) of neutrons impinging on the shielding nuclear material were studied using FLUKA Monte Carlo package. The rectangular blocks of shielding nuclear materials such as concrete ingredients: cement, sand and water were irradiated with a beam of 14 MeV neutrons and the shielding properties of these materials were investigated using FLUKA Monte Carlo simulation code. The simulation set-up replicates the experimental measurements performed within the nuclear laboratory in the Department of Physics at the University of Cape Town. The comparison of the effective removal cross-section shows a good agreement between experiments and FLUKA. The results from these two approaches show general agreement for sand and cement, but show some minor deviations for water and concrete. The source of these deviations is discussed, along with potential solutions.

FLUKA has been well benchmarked and validated against other Monte Carlo codes. The discrepancies obtained on water and concrete may have occurred from the material properties in the input file. Comparisons of results are presented and the discrepancies and agreements between the two methods are discussed for these target materials. The effective removal cross section of a concrete mix was measured by simulation to be 0.1038 +/- 0.0005 cm^{-1} and by experiment to be 0.1230 +/- 0.0002 cm^{-1} of 14 MeV neutrons. This illustrates a broad agreement between experiment and simulation in the case of concrete ingredients. Validation and comparison of measured and simulated neutron irradiation on concrete ingredients shows good agreement, supporting the use of FLUKA for estimating the neutron transmission into the shielding material.

Key words: Monte Carlo; FLUKA; Concrete; Comparison; Experiments; Simulation, Validation

TABLE OF CONTENTS

LIST OF TABLES

LIST OF FIGURES

LIST OF ABBREVIATIONS

CoMSIRU	Concrete Material and Structural Integrity Research Unit
CUP	Computing Unit Processes
MeASURe	Metrological and Applied Sciences University Research Unit
MC	Monte Carlo
STNG	Sealed Tube Neutron Generator
UCT	University of Cape Town
V&V	Verification and Validation
VRT	Variance Reduction Techniques

1 INTRODUCTION

1.1 Background

This Chapter is intended to introduce the background of the work that was performed in this research study. A brief introduction of Monte Carlo technique as well as code verification and validation is provided. The relationship between theory, experiments and simulations in radiation transport is also provided.

The neutron transport equation is the basic equation used to study the neutron transport process in a medium (Wu, 2017). It is essential to understand neutron transport theory and perform reactor physics analysis. The numerical methods used to solve the neutron transport equation are generally divided into the Monte Carlo methods and the deterministic methods. The Monte Carlo (MC) method can be used to address any complex geometry, and its results can be more accurate than those of the deterministic methods. The MC method can handle neutron transport problems of complex geometry, complex neutron spectrum and anisotropic neutron scattering and has been widely employed in neutron transport calculations of fusion reactors. Currently, the most common codes for neutron transport in fusion systems are based on the Monte Carlo method.

The Monte Carlo method is a numerical method based on probability and statistical theories (Wu, 2017). It can explicitly describe the characteristics of randomly moving particles and the process of physical experiments. In contrast, in the deterministic method, a group of mathematical-physical equations is first built up to explain the physical characteristics of the target system (Wu, 2017). Then, by discretizing the variables including direction, energy, space and time in these equations, an approximate solution can be obtained with numerical calculation.

Verification and validation (V&V) are the primary means to assess the accuracy and reliability of computational simulations. V&V methods and procedures have fundamentally improved the credibility of simulations in several high-consequence fields, such as nuclear reactor safety, underground nuclear waste storage, and nuclear weapon safety (Oberkampf & Trucano, 2007). Although the terminology is not uniform across engineering disciplines, code verification deals with assessing the reliability of the software coding, and solution verification deals with assessing the numerical accuracy of the solution to a computational model. Validation addresses the physics modelling accuracy of a computational simulation by comparing the computational results with experimental results. Code verification benchmarks

and validation benchmarks have been constructed for a number of years in every field of computational simulation (Trucano, et al., 2007). This study will validate the results obtained from the experiments against the results obtained using Monte Carlo methods to confirm reliability of the code.

1.2 Problem Statement

The Department of Physics at the UCT has installed a new fast neutron facility featuring a Sealed Tube Neutron Generator (STNG) to be used for applied nuclear physics research and education. The long-term aim of this facility will be to offer fully characterized neutron energy spectra, yield, and calibrated reference detectors. The potential use for such a facility is wide ranging, from nuclear data measurements to elemental analyses to detector development and calibration (Hutton & Buffler, 2017). With the work that is being performed in the experiments to measure interaction of radiation with nuclear shielding materials, there is a need to validate the reliability of results obtained with a simulation code. The first stage is to set up the simulation geometry that is the same as that of experimental set-up, then make predictions with a computer simulations which later can be verified/compared with the results from the experiments.

The main aim of the present work is to examine the validity of FLUKA code to estimate the shielding parameters for fast neutrons on concrete and its constituents.

1.3 Hypothesis

The use of the Monte Carlo method in radiation transport is an effective way to predict the experimental results of the interaction of radiation with matter. It provides a better understanding of neutron transport through nuclear shielding materials and it can also be used to explain the relationship between theory, experiments and simulations in radiation transport.

1.4 Research Questions

This research aims to answer the following questions:

- Can Monte Carlo based radiation transport simulations accurately predict the experimental results for an equivalent geometry set-up?

- Under what conditions do the experimental results agree with the simulation results in radiation transport?

1.5 Objective

The main aim of this research of neutron transport research is to calculate the neutron distribution in the nuclear materials found in nuclear facilities that are used for shielding. To develop corresponding simulation models and compare them with experimental results to validate the reliability of the software coding.

1.6 Scope

The scope of this study comprises the following:

- Perform Monte Carlo simulation of neutron transport experimental set-up, i.e. neutron beam, sample, and detector set-up,
- Comparison of obtained computational results with experimental results,
- Explain the differences/implications of the results from the two approaches.

1.7 Applicability of the Study

The Monte Carlo method has been widely used as a standard method to perform neutron transport simulations in reactor physics for its distinct features. The biggest advantages of the Monte Carlo method to simulate neutron transport in criticality calculation include potentially exact representation of geometrical configurations and physical phenomena that are important for reactor physics analysis (Sharma, et al., 2019). This means that the Monte Carlo method can perform complicated neutron transport problems in whole-core criticality calculation with arbitrary geometrical complexities and arbitrary physical complexities. These key features and advantages indicate that the Monte Carlo method is a very high-resolution and high-fidelity method for neutron transport simulations, which makes it a potential candidate for the next-generation advanced reactor physics methods. However, one of the biggest disadvantages of the Monte Carlo method is that it is time-consuming for neutron transport simulations, especially for large scale whole-core analysis for realistic reactors.

In recent years, there are numerous works on the investigations of both radiation shielding performances as well as mechanical, structural and physical features of different glass systems (Sharma, et al., 2019). Although experimental studies are the final decision-making stage for scientific research, yet the frequency of applications of helpful numerical methods capable of solving the different physical problems is increasing day by day. Monte Carlo simulations can provide significant contributions during the investigation of best radiation protection properties among the studied chemical combinations by minimizing the amount of time, cost and radiation exposure. Therefore, one of the well-known Monte Carlo codes in the literature, namely FLUKA (Ferrari, et al., 2018), has been employed here for the investigation of various shielding parameters of different materials (Sharma, et al., 2019).

1.8 Outline of the Study

This thesis proceeds as follows:

Chapter 1: The current chapter introduces the work to be done in this research project and also provides motivation to the validation research work being conducted.

Chapter 2: In this chapter, a motivation for running simulation codes is provided, and the collaboration and interrelationship between simulations and experiments is also provided, with the highlight that the two approaches should be complementary. Shielding applications is described, with a mention of concrete as a common material in neutron shielding. A brief description of neutron interaction with matter and the use of Monte Carlo as a suitable method for investigation of radiation interaction with various materials is described. Introduction of FLUKA as a Monte Carlo Package for simulation of neutron transport is also presented.

Chapter 3: This chapter provides a description of the Monte Carlo (MC) methods and also highlights on the increase in the use of MC techniques due to fast increase in computer power per unit cost and the invention of powerful software tools. A further description of the MC codes used for neutron transport is provided and the motivation for selecting FLUKA for the current study.

In Chapter 4 the experimental set-up at the nuclear physics laboratory at UCT is described, with the introduction of STNG neutron sources that was used.

Chapter 5: The procedure of how the FLUKA simulations code was set-up and run in the simulations is discussed in this chapter.

Chapter 6: The generic validation approach as practised in the industry is described and followed by the comparison of results between experiments and simulation (FLUKA).

Chapter 7: Lastly, concluding remarks and recommendations of this study are made in this chapter.

The relation between the various chapters of this document can be illustrated in figure 1.1

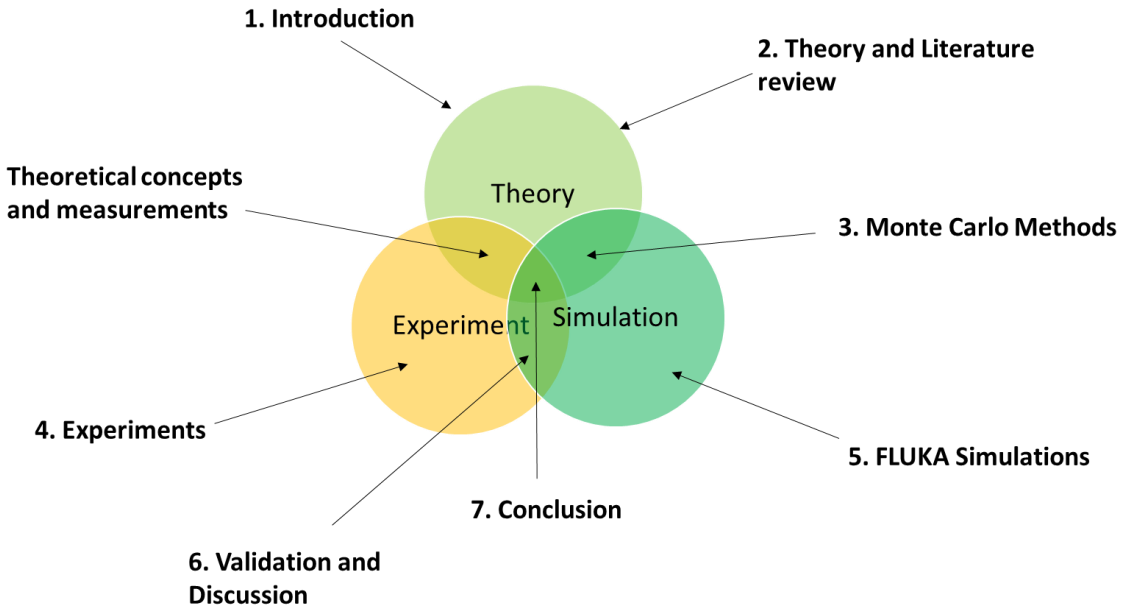

Figure 1.1 Interdependencies of the chapters of this study

2 THEORY AND LITERATURE REVIEW

In this chapter, the theory in the field of neutron transport that is relevant to this research work as well as the literature that outlines work that has been conducted by other researchers that is relevant to the objective of this study are presented.

2.1 Introduction

There has been dramatic progress in the scope and power of computational simulations in recent years; and because codes are generally cheaper to write, to run and to diagnose than experiments, they have a well-recognized potential to extend our understanding of experiments. However, simulations are imperfect models for physical reality and can be trusted only so far as they demonstrate agreement, without bias, with experimental results (Greenwald, 2004). The “validation” process tests the correctness and completeness of the physical model along with the assumptions and simplifications required for solution. The interaction and interrelationship between these approaches has had a profound impact on the quality of research and the rate of its progress. This study discusses the benefits of a close and ongoing collaboration between numerical simulation and experiments, outlines principles and practicalities that are involved (Greenwald, 2004). This chapter aims to provide brief explanation of the theoretical knowledge that the present work is based upon.

Theory and computation on the one hand and experimentation on the other should be seen not as competitive activities but as complementary ones (Greenwald, 2004) . Simulations, though dealing with imperfect models or solutions, can have near perfect diagnostics and are often cheaper and faster than corresponding experiments. The interaction of computation and experiments should not be characterized as simply one of benchmarking a particular code or calculation, but rather should permeate the scientific process and include the mutual identification of interesting or important phenomena, testing of basic physical models and validation of codes and calculations (Greenwald, 2004).

This chapter introduces the basic principles of neutron interactions with matter, neutron transport theory, simulation methods and codes for fusion neutron transport calculations. Furthermore, some evidence is provided on the conducted literature to explore the research questions introduced in section 1.4. In this study, we deal with two different research areas (neutron transport theory and Monte Carlo method) each of which has been studied extensively. At this moment we only provide a brief literature review about neutron transport

theory and, in particular, criticality computations, but we focus more on Monte Carlo methods and Monte Carlo codes. A large amount of literature is available on Monte Carlo method and its applications in neutron transport problems.

2.2 Theory

2.2.1 The neutron transport equation

According to Bergstrom (2013) two methods exist for simulating and modelling neutron transport and interactions in the reactor core, or “neutronics.” Deterministic methods solve the Boltzmann transport equation in a numerically approximated manner everywhere throughout a modelled system. Monte Carlo methods model the nuclear system (almost) exactly and then solve the exact model statistically (approximately) anywhere in the modelled system. Although deterministic methods are fast for one-dimensional models, both methods are slow for realistic three-dimensional problems (Bergstrom, 2013). All particle transport is described by the Boltzmann transport equation in phase space which is a balance between production and destruction of particles during the evolution of time (Bergstrom, 2013).

We now describe the neutron Boltzmann equation, also called the neutron transport equation, to characterize a relatively small number of neutrons colliding in a vast sea of nuclei. Mathematically, a neutron is a neutral point particle, experiencing deflection from or capture by a nucleus at the centre of an atom. The statistically large number of neutrons interacting in a reactor allows for a continuum-like description through averaging resulting in the linear Boltzmann equation (Ganapol, 2008). Also, a statistical mechanical formulation, first attempted by Boltzmann for interacting gases, provides an appropriate description. Boltzmann’s equation, based on physical arguments, such as finite particle size, gives a more physically precise picture of particle-particle interaction (Ganapol, 2008).

As more applications are required of the radiations (e.g. neutrons and photons), be it a nuclear reactor, shielding facility, or a radiation treatment apparatus, the demands on the capability and accuracy of design and analysis are increasing ever to a very high degree (Cho & Chang, 2009). One (perhaps the ultimate) task in designing such a nuclear system is to determine the distribution of the neutrons (and/or photons) in the system under design accurately (Cho & Chang, 2009). For that, we have to take into account the motion of the neutrons and their interactions with the host nuclei of various kinds. Thus, we need a mathematical model or theory to describe this particle transport phenomena.

As a high-level model that describes the distribution of neutrons in a medium such as a reactor, we usually consider the following Boltzmann transport equation (Cho & Chang, 2009):

$$\frac{1}{v}\frac{\partial}{\partial t}\phi(\vec{r},E,\hat{\Omega},t)+\nabla.\hat{\Omega}\phi(\vec{r},E,\hat{\Omega},t)+\Sigma_{\text{total}}(E)\phi(\vec{r},E,\hat{\Omega},t) = \int_0^{\infty}\int_0^{4\pi}\Sigma_s(E'\to E,\hat{\Omega}'\to\hat{\Omega})\phi(E',\hat{\Omega}')d\hat{\Omega}'dE'+S(\vec{r},E,\hat{\Omega},t) \quad 2.1$$

Where the symbols and the terms in the equation are described in table 2.1 below:

Table 2.1 Symbols and terms in the Boltzmann transport equation

Symbol and terms	**Meaning**
$\vec{r}$	is absolute position (vector) (i.e. x,y,z)
E	Neutron Energy
$\hat{\Omega}$	Unit vector (solid angle) in direction of motion
v	Neutron speed (scalar)
$\sum_{Total}$	Macroscopic total cross-section , which includes all possible interactions
$\phi(\hat{r},E,\hat{\Omega},t)$	The angular flux
$\frac{1}{\bar{v}}\frac{\partial}{\partial t}\phi(\hat{r},E,\hat{\Omega},t)$	The time rate of change of neutron density
$\nabla.\hat{\Omega}\phi(\hat{r},E,\hat{\Omega},t)$	Neutron streaming term
$\Sigma_{\text{total}}(E)\phi(\hat{r},E,\hat{\Omega},t)$	Neutron losses due to all types of collisions
$\int_0^{\infty}\int_0^{4\pi}\Sigma_s(E'\to E,\hat{\Omega}'\to\hat{\Omega})\phi(E',\hat{\Omega}')d\Omega'dE'$	Double differential scattering cross section Characterizes scattering of a neutron from an incident energy E' in dE' and direction $\hat{\Omega}'$ in $d\hat{\Omega}$ to a final energy of E and direction $\hat{\Omega}$
$S(\hat{r},E,\hat{\Omega},t)$	Source term

This Boltzmann transport equation is used to describe neutron distributions in details inside the reactors, which can be in the form of spatial distributions, energy distributions and directional distributions. The solution to this equation involves seven dimensional phase space

i.e. angle, energy space and time, with co-ordinates $x, y, z, E, \Omega_{\phi}, \Omega_{\theta}, t$, with the appropriate initial and boundary conditions provided. The use of Monte Carlo is highly recommended in this regard. Below is a list of assumptions that are made when solving equation 2.1 (Cho & Chang, 2009):

i. The medium is isotropic (e.g., the medium exhibits no polarization of neutrons),
ii. The neutrons are emitted isotropically,
iii. All neutrons are emitted promptly (this can be relaxed by considering that some neutrons are delayed), and
iv. The neutron is a point particle that is described classically by its position and velocity.

The cross-sections (the degrees of various reactions) are given by experimental data or by theoretical calculations, if experimental data are not available, with the help of quantum mechanics. The problem of finding solutions to Eq (2.1) is nontrivial or defies elementary approaches of analytical methods, but requires sophisticated numerical methods. This is due to i) the complicated energy and space-dependency of the cross sections, ii) the angular dependency of the scattering cross section, and iii) complexity due to the $\Omega.\nabla\phi$ term, particularly in curvilinear coordinates (Cho & Chang, 2009).

2.2.2 Variance reduction techniques

In this sub-section we describe a technique for improving on the speed and efficiency of a simulation, usually called “variance reduction techniques.” A number of variance reduction techniques have been implemented in the majority of the state-of-the-art Monte Carlo computational tools, aiming at reducing the uncertainty of the computed results by means of using weighting techniques and importance criteria, among others, and giving rise to non-analog Monte Carlo techniques (Kleijnen, et al., 2010).

Kleijnen (2010) stated that Monte Carlo methods are simulation algorithms to estimate a numerical quantity in a statistical model of a real system. These algorithms are executed by computer programs. Variance reduction techniques (VRT) are needed, even though computer speed has been increasing dramatically, ever since the introduction of computers. This increased computer power has stimulated simulation analysts to develop even more realistic models, so that the net result has not been faster execution of simulation experiments; e.g., some modern simulation models need hours or days for a single ’run’ (one replication of one scenario or combination of simulation input values) (Kleijnen, et al., 2010). Moreover, there are some simulation models that represent rare events which have extremely small

probabilities of occurrence), so even modern computer would take 'for ever' (centuries) to execute a single run-were it not that special VRT can reduce theses excessively long runtimes to practical magnitudes (Kleijnen, et al., 2010).

The application of Variance Reduction Techniques in Monte Carlo (MC) codes brings significant improvement in efficiency and a significant profit in the time of simulation. Monte Carlo methods are simulation algorithms used to estimate a numerical quantity in a statistical model of a real system and it is practical and accurate way to simulate experiments that would be difficult or impossible to carry out (Mohammed, et al., 2016). As the Monte Carlo method is statistical in nature, it is possible to estimate statistical errors (variance) of the results gained which are based on the number of simulated events (Mohammed, et al., 2016). Acquiring results with low errors necessitate a long computation time, therefore several algorithms have been introduced to shorten simulation. Variance reduction techniques are algorithms that lead to simplify the calculating or reducing the time and the variance (statistical error) of simulation (Mohammed, et al., 2016).

Employing of variance reduction techniques in Monte Carlo code leads to improve the efficiency of simulation, in other words reducing the Computing Unit processes (CUP) time of simulation and statistics error. According to Louvin (2017), there are three ways for a variance reduction technique to modify the simulation:

- To control the particle population, by increasing/decreasing it in areas of high/low interest;
- To modify the occurrence probability of certain physical processes in order to increase the probability for a particle history to contribute to the score;
- To replace parts of the Monte Carlo simulation by deterministic calculations to improve the overall computation time.

2.2.3 Interaction of neutrons with matter

The use of materials for radiation shielding applications is increasing day-by-day for medical, reactors, accelerators, industries, agriculture, space, etc. The choice of materials selection is dependent upon the requirement for exposure rate reduction, type of radiation, space constrains and final cost effective analysis. Cement, gypsum and lead are common and very useful materials in the field of nuclear engineering for shielding applications (Sariyer, et al., 2015). These materials are being used for the purpose of construction of nuclear facilities and

direct shielding applications. Below are some of the studies on radiation shielding that utilize the Monte Carlo methods:

a) "Multi-objective optimization strategies for radiation shielding performance of BZBB glasses using Bi_2O_3: A FLUKA Monte Carlo code calculations" by Mostafa et al (2020)

In this study, a wide-range investigation on gamma shielding properties of xBi_2O_3-$30B_2O_3$-(65-x) ZnO-5BaO in terms of their potential utilization for radiation shielding aims was presented. The simulation values by Monte Carlo code (FLUKA) have been shown to converge and correlate with XCOM values. The investigated glasses were coded as BZBB1, BZBB2, BZBB3, BZBB4, and BZBB5. As a first step, an essential radiation shielding parameter entitled mass attenuation coefficients (MAC) were extensively calculated in the energy range of 0.015 MeV–15 MeV via a code namely FLUKA. That indicates to the addition of Bi_2O_3 improves the radiation shielding properties of BZBB glasses.

The obtained results were compared with the most commonly shielding materials such as lead and concretes. Further, the obtained results have been compared with the XCOM program data. The comparison showed that there is a well-agreement between the obtained results. It can also be concluded that Bi_2O_3 reinforcement has a synergetic impact on nuclear shielding properties of this type of glass system. It was concluded that the improved BZBB glasses with the addition of Bi_2O_3 showed excellent shielding properties comparing with shielding materials. These results could be highly beneficial for fields such as medical treatment facilities. Therefore, potential investigations on higher additive amounts of Bi_2O_3 and their direct impact on nuclear shielding properties can be considered as the main theme for further studies. It can be concluded that the BZBB5 glass sample can be considered for any industrial development for its implementation in radiation shielding aims.

b) "Simulation of shielding parameters for TeO_2-WO_3-GeO_2 glasses using FLUKA code" by Sharma, et al 2019

This paper aimed to report the results on the investigation of photon attenuation parameters for TeO_2-WO_3-GeO_2 glasses using FLUKA Monte Carlo code. In order to test the validity of the present code, the computational values of mass attenuation coefficients have been in confirmation with those of both previously published experimental data (MoO_3-B_2O_3-Bi_2O_3) and XCOM database at various energies between 356 and 1330 keV. The relative deviation between FLUKA and experimental data is below 5.19% while the difference between the present code and XCOM database is found to be almost 2%. Therefore, the estimated results are in good agreement to each other and exhibited that FLUKA simulation is an alternative technique in determining the shielding performance of the present glass system.

The validity of the physical models applied in FLUKA Monte Carlo code has been benchmarked for selective glass samples for some useful energy values. Firstly, the results obtained by FLUKA are tested against previously reported experimental data for MoO_3-B_2O_3-Bi_2O_3 glasses and it was found that FLUKA results are very close to experimental data. These findings indicate that FLUKA simulations can be a good choice in estimating the radiation shielding parameters of glasses. Thereafter, the difference between FLUKA code and XCOM data base for TeO_2-WO_3-GeO_2 system has been calculated and found to be lower than 0.7% with exception at 1330 keV for TeWGe1 sample. Moreover, MFP and HVL results indicate that TeWGe5 glass sample has the best shielding performance among the selected glasses.

c) "Monte Carlo Simulation of Neutron Transmission of Boron-Alloyed Steel" by Bastürk, et al

Boron is the important absorber used for the production of boron-alloyed steel to serve in long-term storage of spent nuclear fuel or nuclear waste disposals. Due to the high neutron absorption of boron compared to steel, the neutron radiography is a powerful tool for the non-destructive investigation. The study concerns quantitative estimations of secondary effects on the neutron transmission measurements through thermal neutron shielding materials such as beam hardening, background, and inhomogeneous absorber distribution within the samples, which decrease the neutron attenuation in absorber materials. Neutron transmission measurements have been performed for boron-alloyed steel plates having different thickness using thermal neutrons.

The attenuation coefficients of boron-alloyed steels were measured with neutron radiography and the special neutron transmission set-up "JEN-3," which is used for routine test measurements of shielding materials by the Austrian Steel Production Company Böhler Bleche GmbH. In addition to the transmission measurements, Monte Carlo Neutron Particle (MCNP) simulations were performed for better understanding and interpretation of the obtained experimental results. This is the first step of the study covering the estimation of some secondary effects on the neutron transmission. Further experiments will be continued using different absorber materials and homogeneity distribution in order to verify afore said factors in the transmission experiments of neutron shielding materials.

The measured neutron attenuation coefficients show clear differences after a specific thickness of material, which can be called a detection limit. The estimated effective factors responsible for this deviation have been analysed with the help of the MCNP code. The good agreement between the experimental and simulated data allows estimating the contribution of the beam hardening and also neutron multiple scattering effects to the radiography image.

For a good shielding material, the absorber such as boron should be distributed homogeneously.

d) “Photon and neutron shielding performance of boron phosphate glasses for diagnostic radiology facilities” by Tekin, et al (2019)

This study focused on radiation shielding characteristics of Li_2O, Al_2O_3 and ZnO-doped boron phosphate glasses containing PbO and Bi_2O_3. Mass attenuation coefficient (μ/ρ) values of the glasses have been calculated using MCNPX code at various photon energies ranging from 60 to 120 keV and compared to those of XCOM software. The obtained results exhibited that MCNPX and XCOM are in good agreement at all energies. Some shielding parameters such as effective atomic number (Z_{eff}), effective electron density (N_{el}), half value layer (HVL), mean free path (MFP) and Photon transmission factors (TF-photon) were determined using the obtained mass attenuation coefficients. Moreover, macroscopic effective removal cross sections (Σ_R) and neutron transmission factors (TF-neutron) for fast neutrons have been evaluated.

It was then found that Monte Carlo simulation is a suitable method for investigation of radiation interaction with materials in various literature as described in these studies.

Different materials such as hydrogen, iron, graphite, water, polyethylene and concrete have suitable scattering cross-sections and hence can be used for moderating fast neutrons. Concrete is one of the most appropriate and common stuff in composing of neutron shield. There are also various options in using material in producing it that result in composition of concrete material with different densities and compounds for benefiting from proper structural properties (Sariyer, et al., 2015).

Concrete is the most generally used shield material as it is inexpensive and adjustable for any construction design. Radiation shielding properties of concrete may vary depending on the concrete composites. According to the simulation results conducted by Sariyer (2015), adding different proportions of boron carbide and Ferro-boron to concrete can enhance its neutron shielding properties. However, Ferro-boron added to concrete becomes more effective in shielding neutrons than boron carbide added to concrete. According to the simulations results conducted by Sariyer (2015), concrete by adding different proportions of boron carbide and Ferro-boron can enhance neutron shielding property and Ferro-boron added to concrete is the effective of neutron shielding from boron carbide added to concrete.

For shield-design purposes, radiation interactions with matter are simulated easily using various Monte Carlo packages (Sariyer, et al., 2015), such as FLUKA (Ferrari, et al., 2018), GEANT4 (Agostinelli, et al., 2003), MCNPX (Pelowitz, 2011) MARS (Mokhov & James, 2017), and PHITS (Sato, et al., 2013.) etc. FLUKA is a fully integrated particle physics Monte Carlo simulation package. It is a code based on the FORTRAN programming language. Areas of applications of FLUKA code are as follows; high energy experimental physics and engineering, shielding, detector and telescope design, cosmic ray studies, dosimetry, medical physics and radio – biology (Ferrari, et al., 2018).

Hydrogenated materials such as concrete or water are very effective in the moderation of neutrons. Hydrogen in concrete is known to be a radiation protection (especially neutron) process. Concrete blocks absorb neutrons due to hydrogen content. Neutrons are slowed down by thermal energy with hydrogenous materials. These materials are usually water, paraffin and plastic. One of the best materials used in neutron shielding is water because it is even more homogeneous than the best shielding material (Uğur, 2017).

2.2.4 Effective macroscopic removal cross-section

The application of a biological shield between a source of radiation and the personnel resolves the problem of protection of radiation workers against ionizing radiation (Sahadath, et al., 2017). Neutrons are used in many industrial/medical researches and can be produced by different nuclear reactions. Neutron sources can be classified as nuclear reactors, radioisotopes, and particle accelerators. The neutrons emitted are mostly high energy neutrons which are known as fast neutrons in the order of MeV. The fast neutrons are more difficult to shield because absorption cross-sections are much lower at higher energies. Thus fast neutrons must first be thermalized either by elastic or inelastic scattering. In general, an efficient neutron shield is a combination of hydrogenous or low mass number materials to moderate neutrons; high absorption cross section materials to absorb the thermal neutrons and high atomic number materials to absorb the generated gamma-rays (Sahadath, et al., 2017). According to Sahadath (2017), several investigators have contributed to find the neutron shielding properties of concretes and building materials, different types of resin, different polymers, compounds, borate glasses, and multilayered biological shields.

For neutron attenuation calculations, the elastic and inelastic scattering reactions, and neutron capture interaction processes, are of great importance. The effectiveness of the sample of the shielding material can be described by an equivalent absorption cross section, called the effective removal cross section (Sahadath, et al., 2017). The effective removal cross section

for fast neutrons is often used to help in the design of shielding in nuclear facilities. This parameter is used to characterize the attenuation of fast neutrons in materials (Elmahroug, et al., 2013).

Radiation shielding involves placing a material between the ionizing radiations source and the worker or the environment. The radiations which have to be considered are: x and gamma rays, alpha particles, beta particles, and neutrons, each type of these radiations interacts in different ways with shielding material. Therefore, the effectiveness of shielding varies with the type and energy of radiation and also varies with the used shielding material. However, the focus of this study is mainly on the shielding of neutrons. The best materials for protection against ionizing radiation are a mixture of hydrogenous materials (polyethylene, water and many plastics) and neutron absorbing elements (B, Li, Bi, Cl, etc.). This is because they reduce both the intensity of gamma rays and neutrons. Hydrogen slows fast and intermediate neutrons energy via inelastic scattering, and they become thermal neutrons which are absorbed by neutron absorbing elements which have a very high neutron absorption cross-section (Elmahroug, et al., 2013).

Neutron penetration in shielding is characterized by several parameters such as the effective removal cross-section, the macroscopic thermal neutron cross section. In this study, the macroscopic effective removal cross-section of fast neutrons is calculated analytically from simulation and experimental results.

Neutrons are electrically neutral particles; during their passage through a material medium, they interact with the nuclei of atoms in two ways, either by scattering or absorption. The interaction of neutrons with the atoms described by the total microscopic cross-section σ_T (cm^2), expresses the probability that a neutron of a given energy interacts with the atoms of the traversed material, and it is defined as the sum of the microscopic scattering cross-section σ_s and the microscopic absorption cross-section σ_a (Elmahroug, et al., 2013).

$$\sigma_T = \sigma_s + \sigma_a \tag{2.2}$$

The attenuation of neutrons during their passage through material medium depends not only on the microscopic cross-section but also on the number of nuclei within this environment. The physical quantity bound these two parameters, called total macroscopic cross-section denoted $\sum_T$(E) and defined by (Elmahroug, et al., 2013):

$$\sum_T = N\sigma_T \tag{2.3}$$

$$= \frac{\rho N_A}{M} \sigma_T$$

where ρ is the density (g cm^{-3}), N_A is Avogadro's Number and M is the atomic mass. $\sum_T$ has the dimensions of the inverse of the length, their unit is cm^{-1}.

In the same way as a beam of photons, when the parallel beam of monoenergetic neutrons passes through a material medium, it will be attenuated due to absorption and scattering. The attenuation of neutrons in matter follows the following law (Elmahroug, et al., 2013):

$$I(E) = I_0(E) e^{-\Sigma_T t} \quad (2.4)$$

where $I_0(E)$ and $I(E)$ are the incident and attenuated neutron intensities respectively, $t(cm)$ is the thickness of the material medium and $\sum_T$ (cm^{-1}) represents the total macroscopic cross-section.

The case of fast neutron attenuation is described by another parameter called the "removal cross-section", denoted by (cm^{-1}) and is different from the total macroscopic cross-section but it has a fraction of it because not all neutrons are removed from the beam when they interact. The removal cross-section presents the probability that a fast neutron undergoes a first collision, which removes it from the group of penetrating uncollided neutrons. If concrete contains sufficient moderating material, the attenuation of neutrons will be determined by this removal process (Sahadath, et al., 2017).

For energies between 2 and 12 MeV, the effective removal cross-section will be almost constant and when the traversed medium contains a large amount of hydrogen, $\Sigma_R(E) = \Sigma_T(E)$, and when materials contain a small fraction of hydrogen , $\Sigma_R(E) = \frac{2}{3}\Sigma_T(E)$ *for* energy between 6-8 MeV (Elmahroug, et al., 2013) and (El Abd, et al., 2017).

Generally, shielding materials are chemical compounds or mixtures, their macroscopic removal cross-section is calculated from the value of their constituent elements, with the knowledge of the weight percentages w_i, and the values of $(\Sigma_R)_i$ for each of the consisting elements and it is given by the following formula (El Abd, et al., 2017) and (Elmahroug, et al., 2013):

$$\Sigma_R = \sum i \, w_i(\Sigma_R) \quad (2.5)$$

The transmission factor for fast neutrons have been calculated using the attenuation equation as follows:

$$I(E)/I_0(E) = e^{-\Sigma_R t} \tag{2.6}$$

As can be seen, this equation is in exponential form, which can be converted into linear form by taking the logarithm on both sides of the equation, then equation 2.6 becomes:

$$ln\left(\frac{I}{I_0}\right) = -\Sigma_R t + C \tag{2.7}$$

In this linear equation, $\sum_R$ and c represent the gradient and the intercept of the linear equation respectively, which were determined using weighted linear least squares fit. To take into account situations in which the uncertainties in the y- values from point to point, the weighted least square is used when fitting a line to the data. In order to be able to write the equation for m the gradient and c the intercept in a more condensed form, Δ is introduced, which is given by:

$$\Delta = \sum \frac{1}{\sigma_i^2} \sum \frac{x_i^2}{\sigma_i^2} - \left(\sum \frac{1}{\sigma_i^2}\right)^2 \tag{2.8}$$

The remaining quantities can be written in terms of Δ as follows:

$$m = \frac{\Sigma\frac{1}{\sigma_i^2}\Sigma\frac{x_i y_i}{\sigma_i^2} - \Sigma\frac{x_i}{\sigma_i^2}\Sigma\frac{y_i}{\sigma_i^2}}{\Delta} \tag{2.9}$$

$$\sigma_m = \left(\frac{\Sigma\frac{1}{\sigma_i^2}}{\Delta}\right)^{\frac{1}{2}} \tag{2.10}$$

$$c = \frac{\Sigma\frac{x_i^2}{\sigma_i^2}\Sigma\frac{y_i}{\sigma_i^2} - \Sigma\frac{x_i}{\sigma_i^2}\Sigma\frac{x_i y_i}{\sigma_i^2}}{\Delta} \tag{2.11}$$

$$\sigma_c = \left(\frac{\Sigma\frac{x_i^2}{\sigma_i^2}}{\Delta}\right)^{\frac{1}{2}} \tag{2.12}$$

where σ_m and σ_c represent uncertainties in the gradient (m) and the intercept (c) respectively.

The values of the removal cross-section for experiments and FLUKA together with their uncertainty were determined by applying equations 2.8 through to 2.12 to the experimental and simulation data in excel spreadsheet. The obtained results are shown in chapter 6 for water, sand, cement and concrete, and they show good agreement between the FLUKA and Experiments.

2.3 Literature Review

2.3.1 Verification and validation of simulation model

Simulation models are increasingly being used to solve problems and to aid in decision-making. The developers and users of these models, the decision makers using information obtained from the results of these models, and the individuals affected by decisions based on such models are all rightly concerned with whether a model and its results are “correct.” This concern is addressed through model verification and validation. A model should be developed for a specific purpose (or application) and its validity determined with respect to that purpose. If the purpose of a model is to answer a variety of questions, the validity of the model needs to be determined with respect to each question. Numerous sets of experimental conditions are usually required to define the domain of a model’s intended applicability. A model may be valid for one set of experimental conditions and invalid in another (Sargent, 2011). A model is considered valid for a set of experimental conditions if the model’s accuracy is within its acceptable range, which is the amount of accuracy required for the model’s intended purpose.

Assessment of predictive models has been divided into two distinct activities, verification and validation, with formal definitions and recommended practice for their application. Verification and validation are essentially confidence building activities, aimed at improving the quality of predictions from simulations (Sargent, 2011).

Verification assesses the degree to which a code correctly implements the chosen physical model and is essentially a mathematical problem. Sources of error include algorithms, numerics, spatial or temporal gridding, coding errors, language or compiler bugs, convergence difficulties and so forth. Validation assesses the degree to which a code describes the real world. It is a physical problem and one without a clearly defined endpoint. The relation between the various processes can be illustrated in figure 2.1. Verification should, in principle, precede validation. Comparison between experiments and incompletely converged or otherwise

inaccurate solutions are at best useless and at worst misleading. Agreement with experiments might be fortuitous, causing researchers to neglect critical tests (Greenwald, 2004).

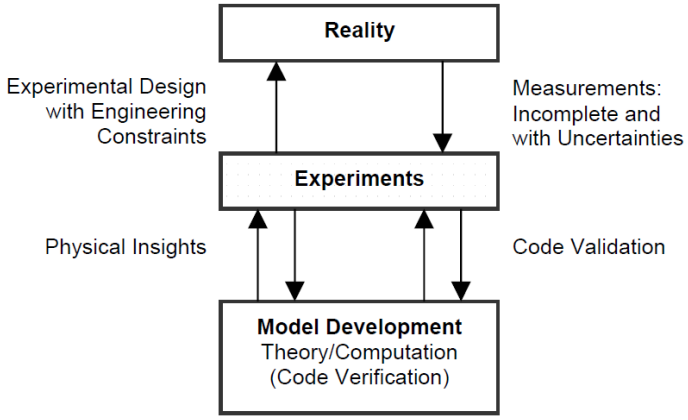

Figure 2.1 Interrelationship of simulations, experiments and physical reality (Greenwald, 2004)

Thus, as computer simulations are given a more central role in the decision-making process, it is believed the credibility of the computational results must be raised to a higher level than what has previously been considered acceptable. Developers of computational software, computational analysts, and users of the computational results face a critical question: How should confidence in computational science and engineering (CS&E) be critically assessed? Verification and validation (V&V) of computational simulations are the major processes for assessing and quantifying this confidence. Briefly, verification is the assessment of the software correctness and numerical accuracy of the solution to a given computational model (Trucano, et al., 2007). Validation is the assessment of the physical accuracy of a computational model based on comparisons between computational simulations and experimental data.

Validation benchmarks are much more difficult to construct and use than verification benchmarks. The primary difficulty in constructing validation benchmarks is that experimental measurements in the past have rarely been designed to provide true validation benchmark data (Trucano, et al., 2007).

2.3.2 Benchmarking of FLUKA with experiments

One straight forward method for validation is comparing data acquired from simulations with experimental results for equivalent setups. Another approach is validation through comparisons with other already validated Monte Carlo code. FLUKA has been heavily benchmarked and validated for many different applications (Engdahl, 2015). The approach used in this project aims to validate the use of FLUKA with experimental data for high energy neutron beams and hence provide additional decision basis for deeming FLUKA appropriate for continued internal use. The study approach in this project consisted of first constructing a simulation setup equivalent to the one used in the experiments and subsequently running simulations with scoring techniques tuned to correspond to the actual measurements.

2.3.3 Neutron transport simulation

According to Vaz (2009), the ultimate goal (the vision) in neutron transport simulation consists in performing detailed 3-dimensional, time- dependent, neutral- and charged-particle transport calculations efficiently and accurately. Historically, neutron transport simulation was first attempted successfully by deterministic methods, solving numerically the Boltzmann neutron transport equation in its integro-differential or integral form, presented in section 2.2.1. Considering the angular and spatial discretization, and the energy grouping described in the sequence and inherent to the methodology adopted for solving the Boltzmann transport equation, it turns out that large hardware (computer memory) is required in order to achieve a reasonable spatial discretization of the system geometry and to accurately describe the physics processes and interactions taking place. However, in recent years, the emerging and innovative technological applications requiring the consideration of higher than 20 MeV neutrons did imply analysis of the Boltzmann transport equation in order to incorporate reaction channels (such as (n, xn)) in the balance of neutrons (Vaz, 2009).

3 MONTE CARLO METHODS

An extensive neutron transport theory that is relevant to this research work as well as the literature review on aspects important to this study such as effective removal cross-section and validation of simulation models was presented in chapter two. In this chapter, a more generic introduction of Monte Carlo is presented. Some of the typical Monte Carlo transport simulation codes that can be applied in many fields such as medical physics, radiation transport are mentioned. FLUKA is the selected MC code, and it's capabilities are also presented in this chapter.

There has been an increase in the use of Monte Carlo techniques in the past decades of medical physics and other applications of neutron transport shielding (Engdahl, 2015). This can partially be explained by the fast increase in computer power per unit cost and the invention of powerful software tools.

According to Wu (2017), with the development of science and technology and the improvement of computer performance, the Monte Carlo method was proposed and developed as an independent method and was first applied in nuclear weapon research. The basic idea underlying the Monte Carlo method is as follows: When the solution to a problem is the probability of an event or the mathematical expectation of a random variable, the occurrence frequency of the event or the arithmetical mean of several specific observations of the random variable can be obtained through numerical experiments. Thus, a solution to that problem is obtained. The advantages of Monte Carlo methods include realistic descriptions of the characteristics of objects with stochastic natures, the ability to simulate physical experiments, few limitations on geometric conditions and parallel computing adaptability. The disadvantages of Monte Carlo methods include the slow convergence rate and statistical uncertainty (Wu, 2017).

3.1 Monte Carlo Method

Bergstrom (2013) explained that the Monte Carlo (MC) method is a numerical integration method very well suited to solve multidimensional Boltzmann equation. The MC method solves problems using random sampling of the events from a known probability distribution. To solve the Boltzmann equation, the geometry and the material have to be described for the problem. Then, with a given set of starting particles, each particle is followed through matter and at each

interaction point a random selection is made from the probability distribution describing the physical outcomes (Bergstrom, 2013).

3.2 Monte Carlo Codes

Wu (2017) stated that the Monte Carlo method can handle neutron transport problems of complex geometry, complex neutron spectrum and anisotropic neutron scattering and has been widely employed in neutron transport calculations of fusion reactors. Currently, the most common codes for neutron transport in fusion systems are based on the Monte Carlo method (Wu, 2017). There exist a number of computational Monte Carlo particle transport codes which implement the Monte Carlo method for criticality safety problems, shielding calculations, dose assessments, burn up calculations. These codes can be categorized either with respect to their particle transport capabilities (neutron, gamma, electron, proton, heavy ion) or with respect to its problem solving capability (Shukla, 2015).

Some of the typical Monte Carlo transport simulation codes that can be applied in many fields such as medical physics, radiation transport and others includes: SuperMC, MCNP, TRIPOLI, Serpent, Geant4, FLUKA, PHITS. Each simulations code offers its capabilities. In this study, the simulation code used was FLUKA, which was chosen based on the availability of the software code and the resources from previous training courses. The computer simulations in this project were solely based on the FLUKA Monte Carlo simulation package and the simulations were set up and executed using FLAIR (the FLUKA advanced interface).

FLAIR provides means for building the executable, debugging the geometry, running the code, monitoring the status of one or many runs, inspecting the output files, post processing of the binary files (data merging) and interface to plotting utilities like gnuplot and PovRay for high quality plots or photo-realistic images (Vlachoudis, 2009). The program includes also a database of selected properties of all known nuclides and their known isotope properties as well as reference database of ~300 predefined materials. Last but not least FLAIR is an open source project, featuring an Application Programming Interface (API) for manipulating FLUKA input files, as well all individual components of FLAIR can run as standalone applications, greatly enhancing productivity for expert users and supplying means for organizing everything as batch jobs. To ensure a high quality program and improve reliability, FLAIR has passed all the software testing, verification phases and methods (Vlachoudis, 2009).

3.3 Programming Choices

FLAIR is built entirely using python as programming language and Tkinter for the graphical interface. Python is a well-established interpreted interactive object-oriented language and portable almost on all operating systems. When executing FLAIR through python, the program is initially compiled and optimized in a pseudo-code assembly language and a virtual machine is interpreting this pseudo-code (Vlachoudis, 2009).

Among the various window interfaces the choice for FLAIR was to use Tkinter which is the default graphical user interface widget set for Python. For the plot generation, the wide spread package Gnuplot was used. Gnuplot is a command-line driven, interactive function plotting program specially suited for scientific data representation (Vlachoudis, 2009).

FLUKA is a Monte Carlo code developed for high energy physics. In FLUKA we call neutrons below 20 MeV **low energy neutrons.** For neutrons with energy lower than 20 MeV, Fluka uses its own neutron cross section library (P5 Legendre angular expansion, 260 neutron energy groups) containing more than 250 different materials, selected for their interest in physics, dosimetry and accelerator engineering and derived from the most recently evaluated data (Ferrari, et al., 2018).

3.3.1 Low-energy neutrons in FLUKA

In FLUKA, low-energy neutron transport is activated by an option of LOW-NEUT, but it is requested by defaults with most of the options available with the DEFAULTS command. Command LOW-NEUT may still be necessary in order to give information about the cross section library used, or to issue special requests (Rata, et al., 2016).

3.3.2 Multigroup neutron transport

Transport of neutrons with energies lower than a certain energy is performed in FLUKA by a multigroup algorithm. The energy boundary below which multigroup transport takes over depends in principle on the cross section library used. This energy is 20 MeV for the 260-group library which is distributed with the code (Rata, et al., 2016). In FLUKA, internally there are two neutron energy thresholds: one for high-energy neutrons and one for low-energy neutrons. The high-energy neutron threshold represents in fact the energy boundary between

continuous and discontinuous neutron transport, this is found in the online version of FLUKA (Böhlen, et al., 2014) and (Ferrari, et al., 2005). The multi-group technique, widely used in low-energy neutron transport programs, consists in dividing the energy range of interest into a given number of intervals ("energy groups"). Elastic and inelastic reactions are simulated not as exclusive processes, but by group-to-group transfer probabilities forming a so-called "downscattering matrix" (Rata, et al., 2016).

The FLUKA physics and all possible interactions are explained in detail in the FLUKA manual which can be found on Böhlen,et al (2014) and Ferrari, et al (2005). In FLUKA the Boltzmann equation is solved on an integral form by integration over all phase space coordinates as functions of time, i.e. over each particle history, where the highest number of collision in a history determine the dimension of the Boltzmann equation (Rata, et al., 2016). Each particle is transported through matter and at each integration point the occurrence and outcome from an interaction is randomly selected from the appropriate probability distribution (described either by the implemented physical models or from cross-section libraries for low-energy neutrons).

The statistics can be improved by variance reduction techniques and one simple way in FLUKA is the combination of Splitting and Russian Roulette on boundary crossing by applying relative importance in regions (Rata, et al., 2016). Systematic errors depends on the physical models in the MC code, the algorithms, program bugs and the data uncertainty in the experimental data. It also depends on the implemented geometry, simplifications or missing details as well as the material composition. Even with a correct code the human factor plays its role in e.g. user-defined subroutines, incorrectly built input files, wrong units, incorrect normalization or bad biasing.

3.4 FLUKA Simulations

One of the most important aspects for the FLUKA input is the geometry model that has to be as accurate as possible in order to consider all the potential interactions among particles and matter. FLUKA being a Monte Carlo tool, its algorithms achieve the results by thinking in terms of primary particle, which may be any kind of particle.

In FLUKA the Boltzmann equation is solved on an integral form by integration over all phase space coordinates as functions of time, i.e. over each particle history, where the highest number of collision in a history determine the dimensions of the Boltzmann equation. Each

particle is transported through matter and at each integration point the occurrence and outcome from an interaction is randomly selected from the appropriate probability distribution (Sharma, et al., 2019).

FLUKA Monte Carlo code provides a BEAM input file by which it is possible to choose the particle kind, its energy, its direction and starting position. For more complex situations, generally a devoted ‘user routine’ is preferred (Sharma, et al., 2019).

According to Bergstrom (2013) the geometry description is a set of solid or half-infinite bodies and the regions defined by logical combinations of the bodies. Each region is assigned a material defined in the material settings which is either taken from the FLUKA material database or user-defined. Materials can be single element, isotope or complex compositions. The beam definition describes the particle type, energy, distribution, position and direction of the beam. In the physics settings simulation thresholds can be set (energy, simulation time, particle production and transport). Physical effects not included in the simulations by default can be added. In the scoring definition the output files are configured by choosing the physical quantities of interest and how they should be estimated. Following these configurations is the random number initialization and the FLUKA simulations starts with a requested number of histories (primary particles) and ends when the stop command has been reached (Bergstrom, 2013).

4 EXPERIMENTS

4.1 Introduction to the n-lab

This chapter presents the experimental set-up that was performed which will later be replicated in the simulation set-up. It has to be noted at this stage that the experiments described in this chapter were performed by Msutwana, et al (2019). The results from the experiments are independently analysed and compared with the results obtained from the simulations in the validation and discussion chapter. It may be worth stating that Msutwana's work is an existing data archive containing experimental measurements of the parameters of interest for this study.

Progress in the establishment of a fast neutron beam reference facility for the non-destructive testing of concrete and other materials used in the nuclear industry is described. The project is based on the principle of analyzing the distributions in energy of the neutrons transmitted through the sample. First measurements and analyses of mortar (concrete without large aggregate) using continuous beams of fast neutrons are presented. The measurements and analyses of concrete and its ingredients were presented by Buffler, et al (2019), using continuous beams of fast neutrons and propose avenues of further research.

There have been many studies on the shielding parameters of concrete, most of which have focused on the transmission of gamma rays, and low energy neutrons (Buffler, et al., 2019). There is surprisingly very little work reported using fast neutrons. The concept of an effective neutron-removal cross-section is a useful parameter to express neutron attenuation in hydrogenous media.

The Department of Physics at the University of Cape Town has recently installed a new fast neutron facility featuring a Sealed Tube Neutron Generator (STNG) to be used for applied nuclear physics research and education. Devices such as this are typically used in industrial settings for mining and oil logging, but here the STNG is used as part of the applied nuclear physics teaching and research programs.

4.2 General setup

The 14 MeV STNG source is well shielded in a specially designed and constructed vault, with a beamline extending into the experimental area as shown in Figure 4.1(a). The variable circular collimator is typically operated with a diameter of 0.8 cm at the exit which produces flux of about 400 n/cm^2/s (STNG) at this position. Two detectors are used to monitor the neutron rate and scale each measurement to the same neutron fluence; a liquid scintillator embedded within the vault and near the source, and a thin plastic scintillator at the exit of the collimator. The detector and samples are positioned on a sturdy optical bench. Data sets are acquired in the n-lab within the Metrological and Applied Sciences University Research Unit (MeASURe). A typical measurement layout is shown in Figure 4.1(b). The n-lab has the following schematic layout:

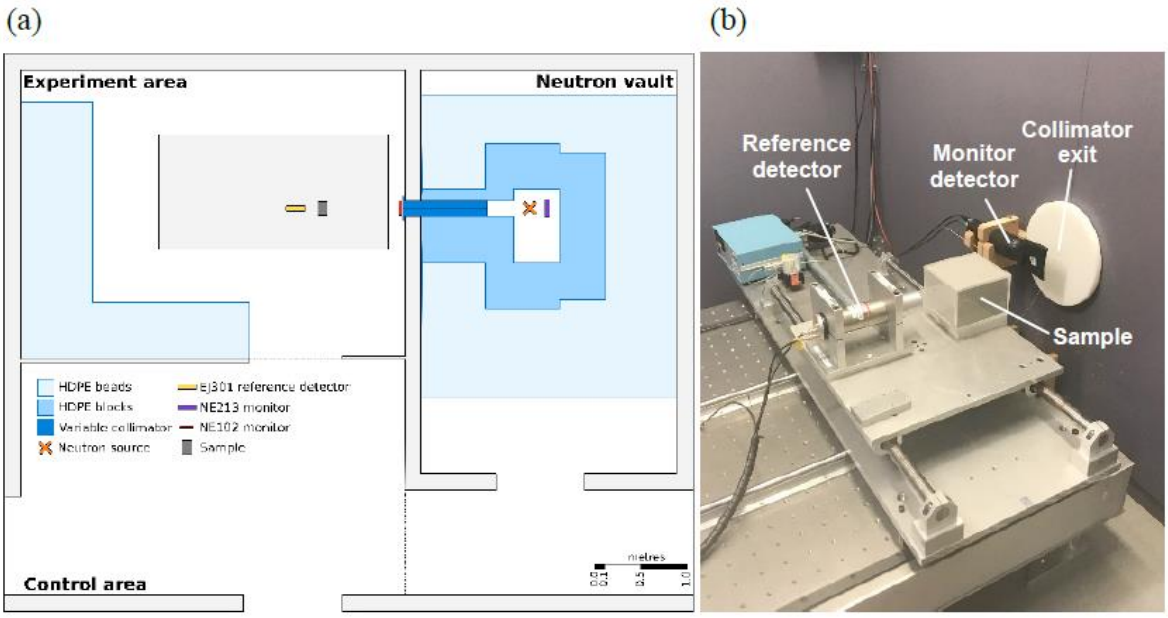

Figure 4.1 Layout of the fast neutron facility (n-lab) at the UCT (Buffler, et al., 2019)

4.3 Method

Neutrons within the energy of 14 MeV are provided by a sealed tube neutron generator (STNG) via the D-T fusion reaction. Measurements of the energy spectra of transmitted neutrons were made for samples of water, sand, cement and concrete for thicknesses ranging from 0 cm to 10 cm. Figure 4.2 shows the geometry of the experimental setup. For the STNG neutron source, the sample is filled with some thickness of material and placed in the setup. At the n-lab, neutrons are incident on the sample from the left on the diagram on figure 4.2, the transmitted neutrons are detected using an organic liquid scintillator detector.

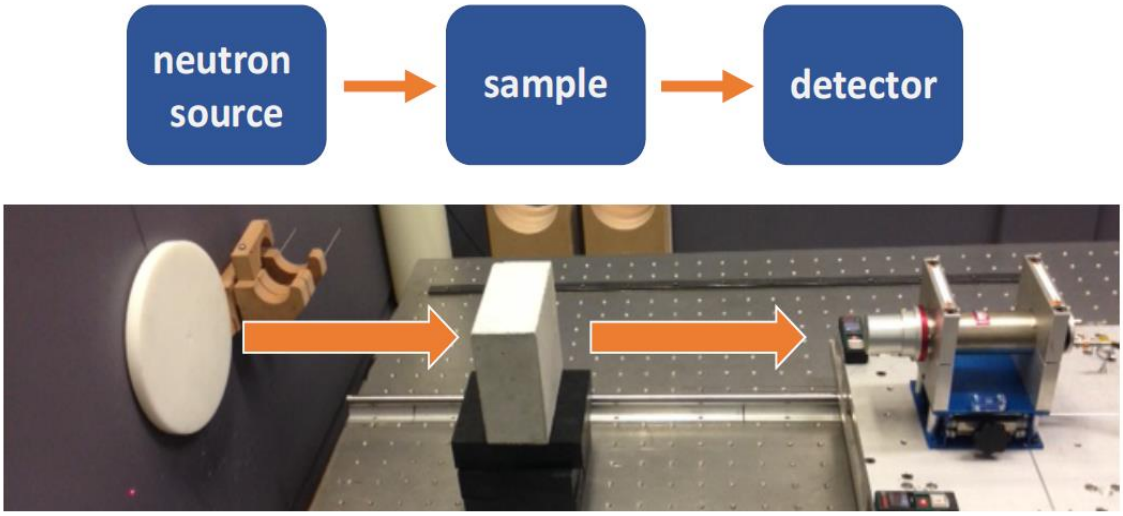

Figure 4.2 Experimental setup in the n-lab

4.3.1 14 MeV STNG (Source)

The neutron source used in the experiment was a 14 MeV sealed tube neutron generator (STNG). This is a Thermo MP-320 sealed tube neutron generator which produces 14 MeV neutron flux energy via the deuterium-tritium fusion reaction. Deuterons are accelerated towards a solid target of titanium embedded with tritium (Hutton & Buffler, 2017).

4.3.2 Samples

Samples for the project are produced by the Concrete Materials and Structural Integrity Research Unit (CoMSIRU) at the University of Cape Town. They were constructed without large aggregate to improve homogeneity of the samples and are thus referred to as “mortar” (Buffler & Hutton, 2020). All samples were manufactured using a Portland cement binder (CEM II/A-L 52.5) with strength grade 52.5, containing approximately 9% of crushed limestone, and an aggregate comprising only standard fine dune sand (calcitic-siliceous, maximum particle size c. 1 mm) as found in the Cape Town area. The water content was reported to be 18.5% by volume at the time of mixing, and the mortar samples were cured in a water bath for 7 days. Mortar samples of identical composition and various thicknesses were

manufactured. All measurements were completed using the same geometry (Buffler & Hutton, 2020).

4.3.3 Material Properties

The sand, cement and concrete samples were subjected to x-ray fluorescence (XRF) analyses with the Department of Geological Sciences at the University of Cape Town. The results are shown in Table 4.1. The uncertainties are reported as being 1% of the values. Of particular note is the high calcium content in the sand sample tested. This is due to naturally occurring variations in composition due to the locality of the sand (Buffler & Hutton, 2020). Cape dune sand has a high proportion of seashell that affects the elemental composition of concrete constructed in the region, and hence the radiation shielding properties.

In table 4.1, H_2O- represents the sample weight lost upon heating the sample powder at 110° for 12 hours. LOI (loss on ignition) represents the weight lost change upon heating the sample to 800°C for 4 hours. Entries indicated with "b.d" correspond to concentrations below the limit of detection (<0.01% by weight) and will have no appreciable effect for neutron interactions in the material.

Table 4.1 Material Properties:

	Sand	**Cement**	**Concrete**
	(weight %)	(weight %)	(weight %)
SiO_2	78.44	18.91	53.50
TiO_2	0.08	0.17	0.10
Al_2O_3	0.37	3.43	1.30
Fe2O3	0.16	2.98	1.03
Mn0	b.d.	0.05	0.02
MgO	0.03	1.40	0.42
CaO	10.83	63.27	24.93
Na_2O	0.23	0.14	0.16
K_2O	0.12	0.58	0.23
P_2O_5	0.04	0.16	0.06
SO_3	0.06	1.91	0.54

Cr_2O_3	b.d.	0.01	b.d
NiO	b.d	b.d.	b.d.
H_2O-	0.24	0.53	4.32
LOI	8.83	5.99	12.47
Sum	99.45	99.55	99.11

4.3.4 Detector

The detector used in the experiments was an EJ-301 organic liquid scintillation detector which was calibrated using standard gamma ray sources. The EJ-301 detector was chosen as it has sufficient neutron γ-ray discrimination, high neutron detection efficiency and good temporal resolution. We use the EJ-301 as a neutron detector, but it is also sensitive to gamma rays. We use gamma rays to calibrate a detector, but otherwise we need to remove them from our neutron measurements via pulse shape discrimination (Msutwana, et al., 2019).

4.3.5 Neutron Transmission

The transmission of directly and indirectly ionizing radiation through matter and its interaction with matter is fundamental to radiation shielding design and analysis (Shultis & Faw, 2010). Transmission factor is obtained from the $I(E)/I_0(E)$ ratio depending on the shield thickness for selected energy range. Transmission factor expresses the ability of neutrons penetrate the material and cover a distance in the material (Tekin, et al., 2019). This parameter is carried out by measuring the amount of radiation from the source by passing the material to determine the required shielding thickness.

In the experiments, the parameters $I_0(E)$ and $I(E)$ represents the intensity measured when there is no sample and the transmitted intensity measured when the sample is in place respectively. In section two the relationship between the neutron intensity and the material thickness was defined, from which the transmission factor was obtained.

5 FLUKA SIMULATIONS

5.1 Introduction

A full description of the selection choice of programming of FLUKA was given in Chapter 3. In this chapter the process of setting up and running FLUKA is presented.

A neutron transport problem that is a direct display/geometry of the experimental set-up presented in Chapter 4 was simulated using Monte Carlo code - FLUKA. The simulations were performed at a simplified model of the experimental set-up, and then later a comparison between the simulation and the experimental results was to be performed. For optimum scientific progress, simulations and experiments must be seen as complementary not as competitive approaches. Further improvements on the agreement between simulation and measurements will be considered. In this chapter, the experimental geometry was replicated in FLUKA, to develop the default geometry set-up. Then different samples of concrete ingredients were introduced into the geometry set-up with some minor modifications in the input file, and then the simulations were performed.

5.2 Geometry

All simulations were based on the default FLAIR input file with the beam, target and detector arrangement shown in Chapter 4. The simulation region is illustrated in Figure 5.1. In this geometry, the beam, target sample and detector were implemented according to the technical drawing in Figure 5.1. The beam line used a 0.8 cm diameter pencil beam of mono energetic 14 MeV neutrons along the positive z-axis, positioned at 0 cm and impinging on a rectangular block (target) that was positioned 24 cm from the beam.

The target consists of a rectangular block with a cross sectional area of 15 cm x 15 cm and variable thickness, filled with water, sand, cement, or concrete. This was henceforth referred to as the default set-up through which the material compositions of the different nuclear materials were specified at different intervals of the simulations. Lastly, the target material was followed by a 5.00 x 5.00 x 2.52 cm^3, cylindrical shaped detector, positioned at 46.5 cm from the beam positon, and scoring the properties of neutrons (number, energy etc.) which pass through this region, as shown in Figure 5.1. Lastly, the geometry set-up was surrounded by a material of Black hole with a radius of 100 000 cm, where neutrons where not counted. All simulations were based on this default set-up, with varying nuclear materials on the target.

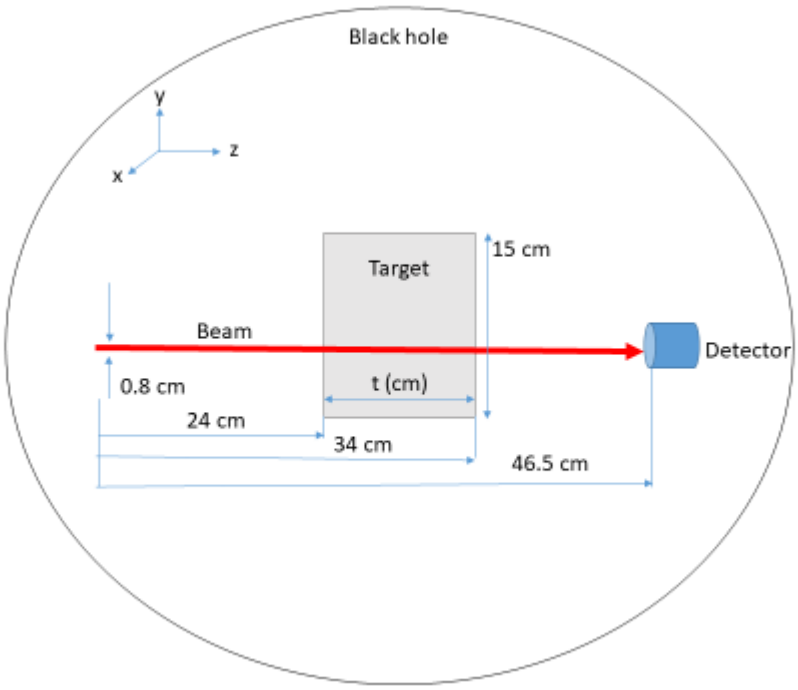

Figure 5.1 Geometry for the simulation which approximates the experimental set-up in figure 4.2, with the 14 MeV neutron beam shown with the red arrow

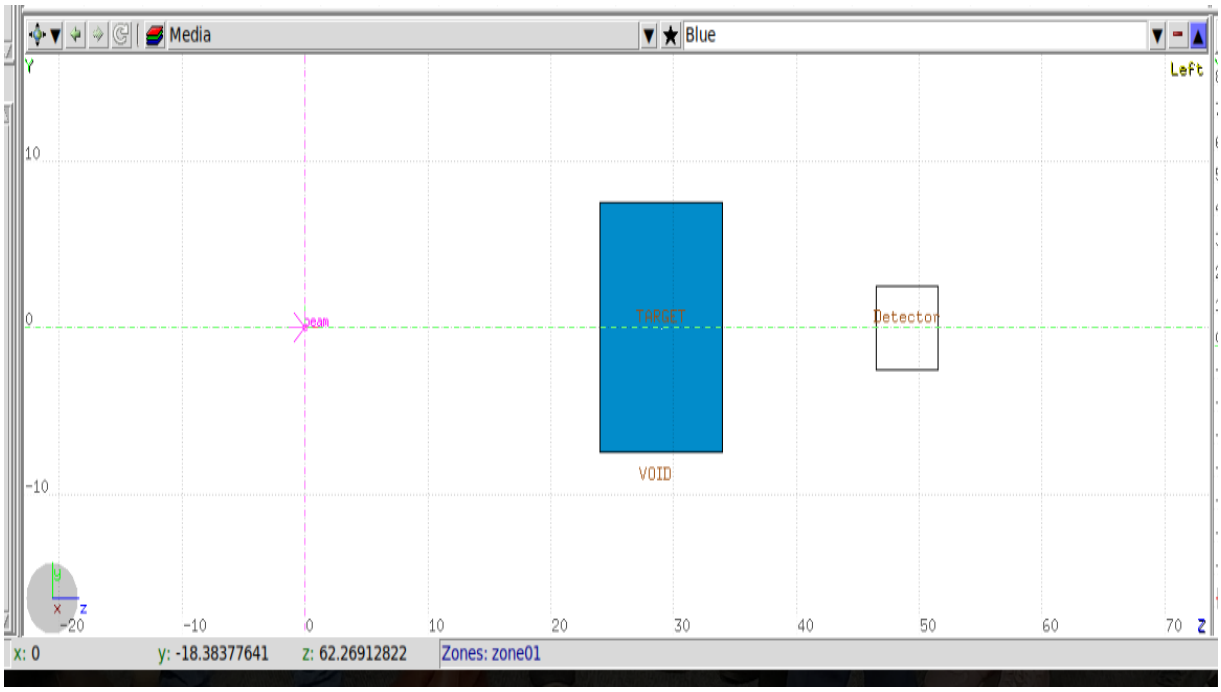

Figure 5.2 Geometry setup for the simulation from Flair (FLUKA), where the neutrons are produced at the origin and are incident on 10.0 cm thick water sample

Figure 5.2 represents the geometry as obtained in the simulation (FLUKA). The figure depicts the source, sample and detector as a default geometry set-up for all materials (water, sand, cement, and concrete).

5.3 FLUKA Input Editor

The minimum requirements for a FLUKA simulation is to define the beam, the geometry, the materials (unless only using the FLUKA material library) and the requested scoring (the MC estimators). The FLUKA input file is a plain text file containing the full description of the particle beam, geometry, materials, physics and scoring as well as the number of primary particles (histories) and executables needed to run a FLUKA simulation. The output files are usually binary and special subroutines are needed to read the outputs and to process and analyze the data. The FLUKA input file is structured as follows:

1. Beam definition
2. Geometry description
3. Material properties
4. Scoring definition (choice of estimators)
5. Initialization of random number
6. START the simulation
7. STOP the simulation

5.3.1 Building the input file in FLAIR

The input file is composed of command lines (so-called input cards) which is the set of lines describing one command or property (e.g. beam specification or a geometry body). In FLAIR the input cards are interpreted as small blocks (or dialogues) for each FLUKA card providing the user with the possible options and with numerical fields when required.

In this section some of these cards, which have been used in the FLUKA simulations presented in this dissertation, are described in more details. The pieces of the input file for each card is also shown.

1. General information

General project information like title, notes, override formatting options for the input file.

2. Beam definition

All cards describing the source and the primary particles are defined here. In the simulation set-up, the particle specified was neutron, with an energy of 14 MeV. The beam position in the simulation set-up was selected to start at zero with respect to x, y, and z. Neutrons were emitted from a point source in a forward direction along the z-axis and the centre of the point source.

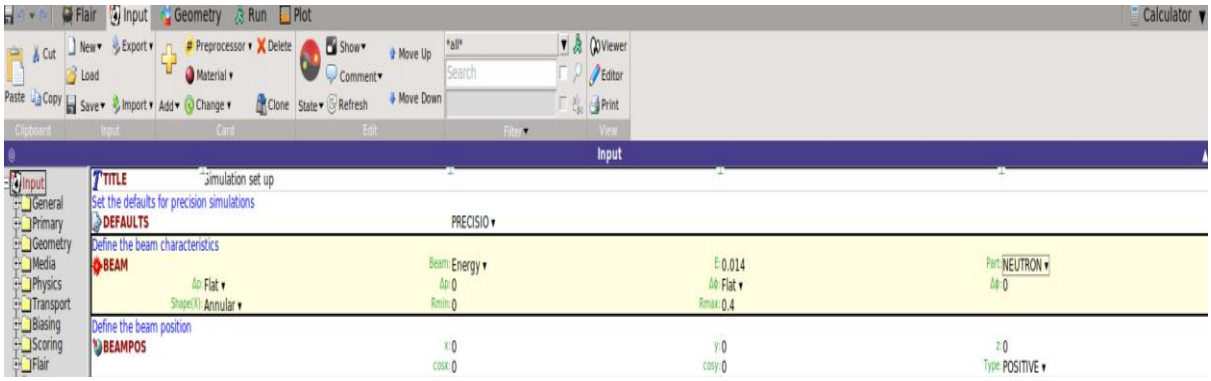

Figure 5.3 Beam characteristics

In figure 5.3 the information on the beam as well as the beam position is shown. The information displayed in the beam energy of 0.014 GeV.

3. Geometry

The geometry set-up was surrounded by a material of Black hole with a radius of 100 000 cm. The Black hole is a fictive material with infinite absorption used to terminate particle trajectories. The space between the Black hole and the set-up was filled with void, radius of 1000 cm. The target was a rectangular parallelepiped box with the dimensions of 15 cm x 15 cm x 10 cm specified as follows, with the z as the horizontal axis measured from the beam position:

Table 5.1 Dimensions in the geometry

Dimensions in the Geometry	
Xmin = -7.5 cm	Xmax = 7.5 cm

Ymin = -7.5 cm	Ymax = 7.5 cm
Zmin = 24 cm	Zmax = 34 cm

This was followed by a detector that was positioned at 46.5 cm from the source (beam) with a radius of 2.5 cm.

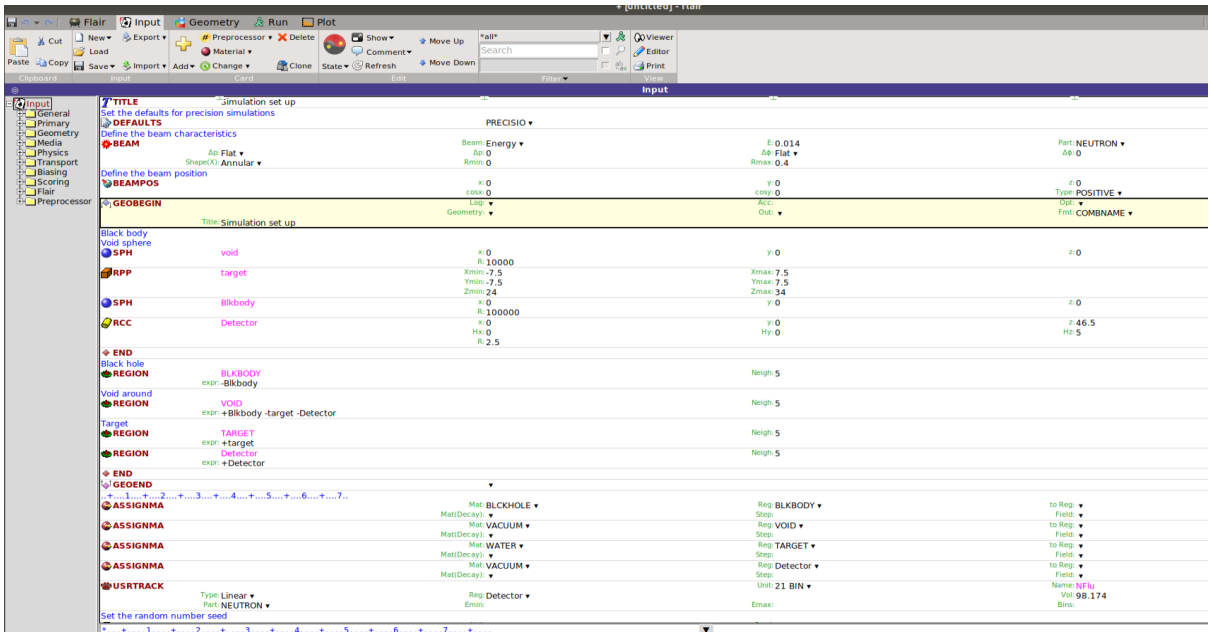

Figure 5.4 Geometry Information

In figure 5.4 the information on the geometry of the simulation as obtained from the input file is displayed. The information displayed in the geometry is the spherical dimensions for the beam, rectangular parallel piped dimensions for the target, spherical dimensions for the black body in which no particle will be counted, and the cylindrical coordinates for the detector.

4. Media

The material assigned for each region were Black-hole for the blackbody, vacuum for the void, water for the target, and vacuum for the detector. The materials for the target were specified for all samples i.e. water, sand, cement and concrete. Material isotopic compositions as well as the compounds for these samples were taken into consideration. This is displayed in the figure below.

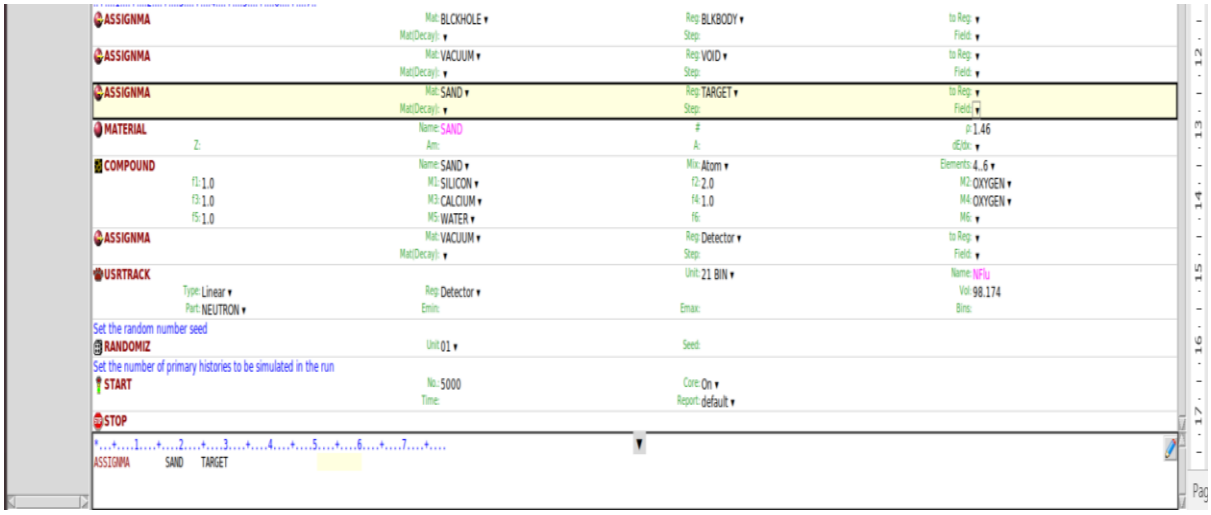

Figure 5.5 Assign Material

5. Scoring definition

The scoring option that was used in the simulation was the USRTRACK. This was used because it calculates differential fluence as a function of energy by scoring track-length in a given region. Resulting histograms are normalized to $GeV^{-1}cm^{-2}$ per primary if the region volume is provided (otherwise should be intended as $GeV^{-1}cm$ per primary, i.e. differential track-length). The region that was scored was the detector and the particles of interest were the neutrons. The volume for the cylindrical detector was calculated using $\pi r^2 h$ to be 98.174 cm^3. The output file from each scoring was chosen in formatted (ASCII) or unformatted (binary) units specifying the unit number.

6. Initialization of random number

Following these configurations is the random number initialization and the FLUKA simulations starts with a requested number of histories (primary particles) and ends when the stop command has been reached. According to Ferrari (2018) all events or histories are initiated by primary particles, which in the case of this research are monoenergetic, monodirectional and start from a single point in space (pencil beam). At the end of the input file, a START card is mandatory in order to actually start the calculation. That card must indicate also the number of particle histories requested. The run, however, may be completed before all the histories have been handled in two cases: if a time limit has been met (on some systems) or if a stop file is created by the user. In the simulation setup the number of primary histories simulated for all the runs was 5000, with 100 cycles for each run.

5.3.2 Running the Simulation

With the Run Frame the user has the ability to run the simulation or create several runs by overriding some parameters. Each run is identified by a unique input name and is based on the same input file (Vlachoudis, 2009). To increase the statistics or to benefit of a multi-core or cluster architecture, the user can submit many runs based on the same input by changing the random number history (Vlachoudis, 2009). FLAIR is monitoring the progress on the run by inspecting the information on the files created by FLUKA, rather than using the process information.

5.3.3 Intensity in the Simulations

In section 2 the relationship between the neutron intensity and the material thickness was described. In the simulations, the energy spectra are used to determine the parameters I_0 (E) and *I(E)*, which represented the fluence (particle per cm^2 per primary) at the energy of 14 MeV obtained from the energy spectra when there was no sample (I_0(E)) and the transmitted fluence obtained when the sample was in place, *I(E)*. The simulations were performed up to a thickness of 10 cm with small increments of 1 cm. At each increment the *I(E)* value that correspond to the energy of 14 MeV was obtained.

6 VALIDATION AND DISCUSSION

6.1 Validation in an Industrial Context

A full description of the experimental set-up and the simulations was provided in chapters 4 and 5. In this current chapter, the comparison (validation) of the results from both approaches is presented and discussed.

Typically, the validation process is presented in a flowchart that splits into parallel strands of activities for computational and experimental modelling and recombines with the quantitative comparison between simulation and experimental outcomes, this is shown in Figure 6.1 (Hack, et al., 2018). Outcomes are compared with the purpose of providing sufficient information for a subsequent decision on whether acceptable agreement of the simulation data with the experimental results has been reached, in which case the model is successfully validated.

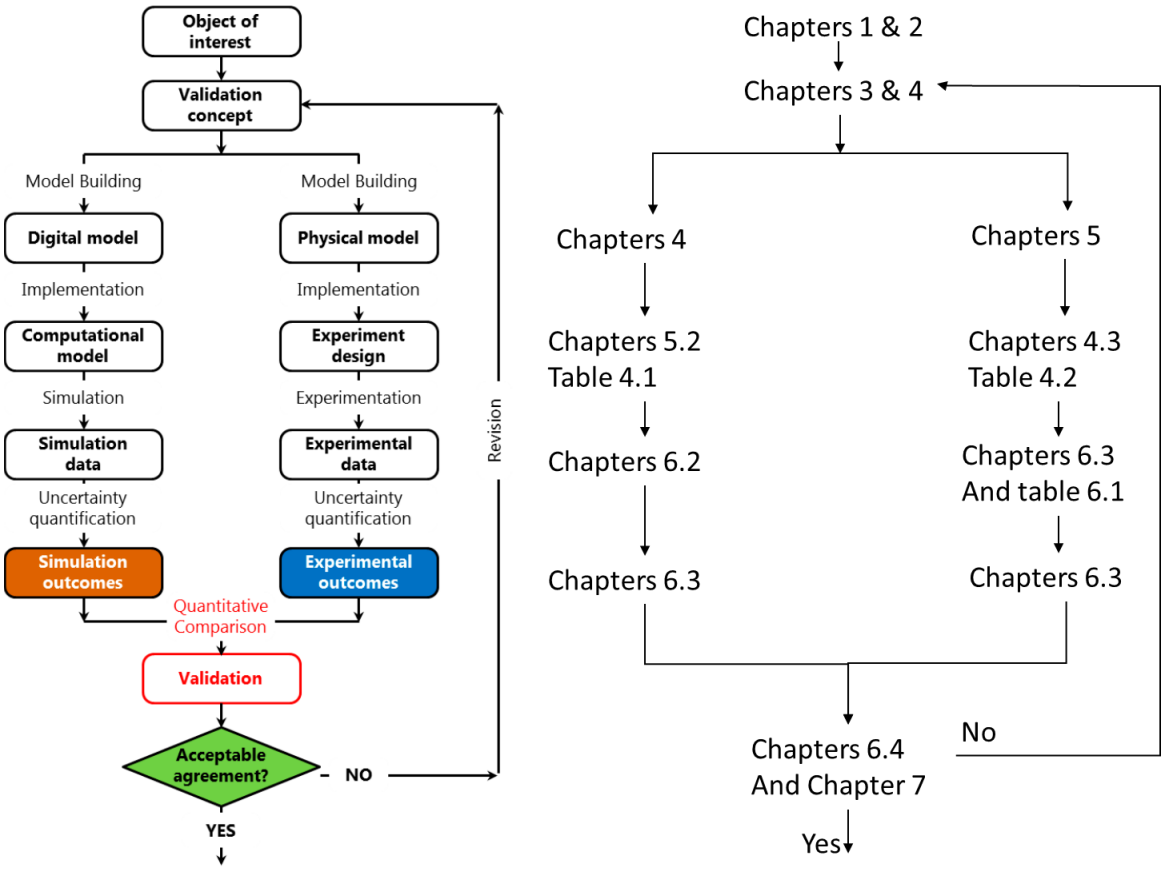

Figure 6.1 Left: A generic quantitative comparison validation flowchart (Hack, et al., 2018). *Right: the relevant sections of the thesis that link to each stage of the flowchart in corresponding positions.*

If the level of agreement is insufficient, then, usually, the computational model or the experiment, or both, need to be reviewed. In general, the process should be repeated until an acceptable agreement is reached (Hack, et al., 2018). To address the specific needs of validation in an industrial environment, the collaboration addresses the following issues, among others. When the experimental results are used as reference against which the computational data are compared in the Validation assessment, insufficient information on the accuracy of the experimental results does not allow adequate confidence to be built for the computational model. This promotes the need for new experiments in order to obtain the necessary information. The acceptable level of measurement uncertainty is governed by the accuracy requirements for the intended use of the model (Hack, et al., 2018).

The flowchart in Figure 6.1 ties together the mathematical and physical strands in the box of quantitative comparison of the simulation results and experimental data. The outcome of this comparison is then assessed in the next step with respect to the accuracy limits, set beforehand, for the intended use of the model. Typically, it is followed by a Yes/No decision as to whether the agreement is acceptable. However, the validation flowchart, places equal emphasis on test and simulation, or experiment and model (Hack, et al., 2018).

6.2 Energy Spectra

To determine the influence of the total transmitted beam caused by the material itself, a series of simulations has been performed using the FLUKA code. Fluence is specified as the number of particles traversing a unit surface in a particular point in void per unit time. The neutron energy spectra presented in figure 6.2 - 6.6 are all histogram data, with the data points plotted at the lower limit of the energy bin.

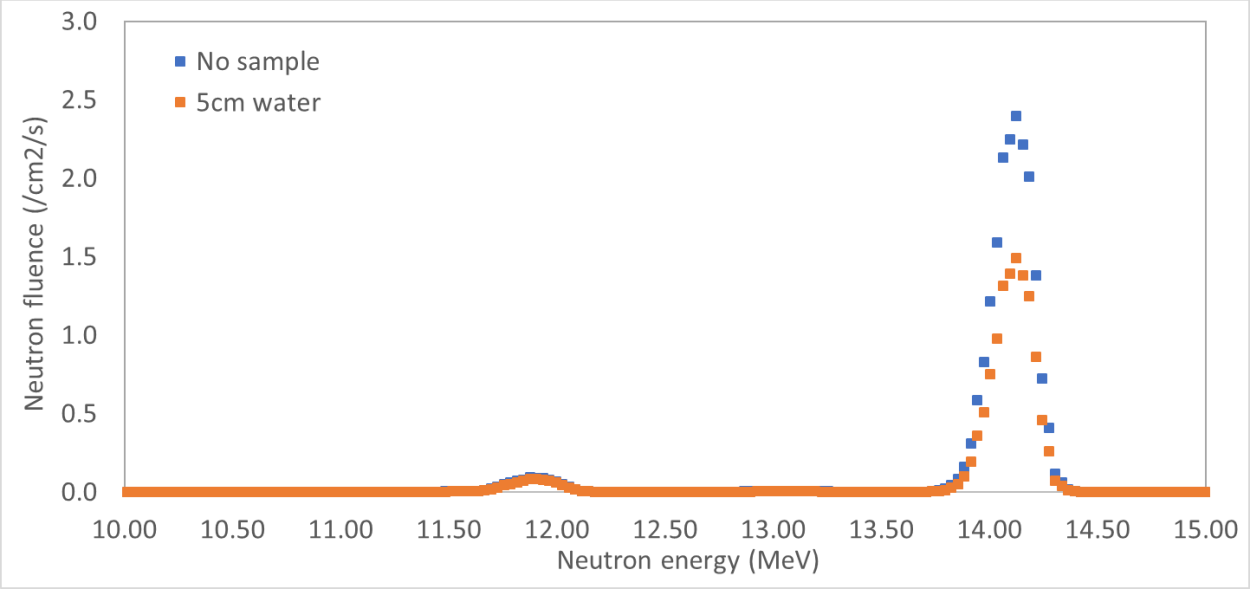

Figure 6.2 Neutron fluence as a function of energy of a 14 MeV neutron as obtained from experiments (Buffler & Hutton, 2020)

The results in figure 6.2 shows the neutron energies at different levels with the peak energy at 14 MeV for both “5 cm water sample” and “no sample” as observed in the experiments. This peak energy represents neutron energy source i.e. the STNG source that was used in the experiments. These results were obtained from the experimental set-ups. The area under the 14 MeV peak was used to calculate $I_0(E)$ and $I(E)$ respectively.

The simulation results for energy spectra were obtained by first scoring the energy dependent neutron fluence spectra with FLUKA. Neutron fluences (particles per cm^2 per primary) as a function of energy (GeV) for different shielding materials from FLUKA are shown in Figures 6.3 – 6.6. The quantity plotted is the energy dependent fluence of neutrons transmitted through the target and incident on the detector. The value of the histogram in the 14 MeV region is used as the $I_0(E)$ and $I(E)$ respectively.

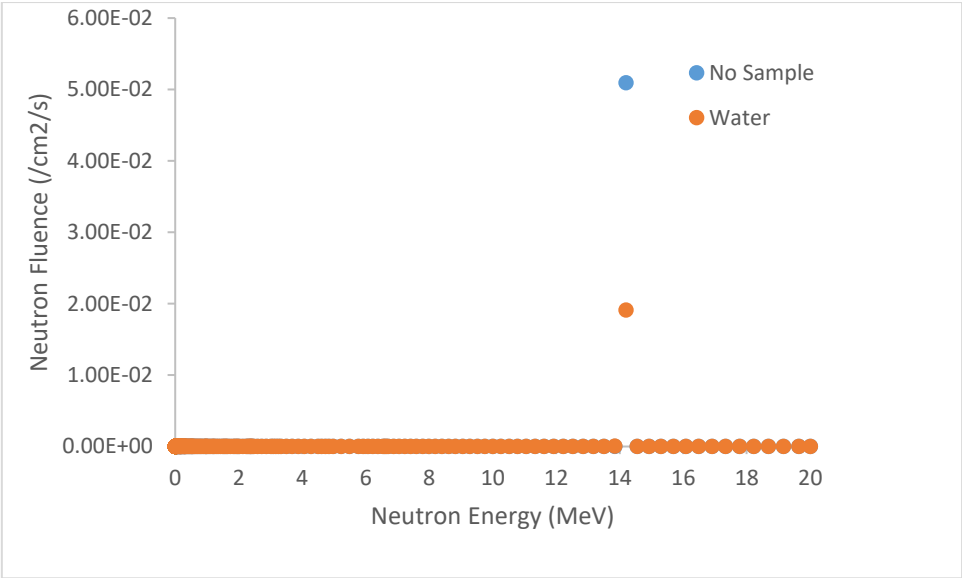

Figure 6.3 Neutron fluence as a function of energy of a 14 MeV neutron incident on water target

The results in figure 6.2 as obtained from the experiments and the results obtained in FLUKA (figure 6.3 - 6.6) may not be compared quantitatively. The shape of the 14 MeV neutron peak is very different in the experimental case compared to the simulation case preventing a direct comparison. This is due to the simplified simulation, were the detector response is not included. However, the relative behaviour (transmission factor) of the experimental and the simulated case can be compared quantitatively.

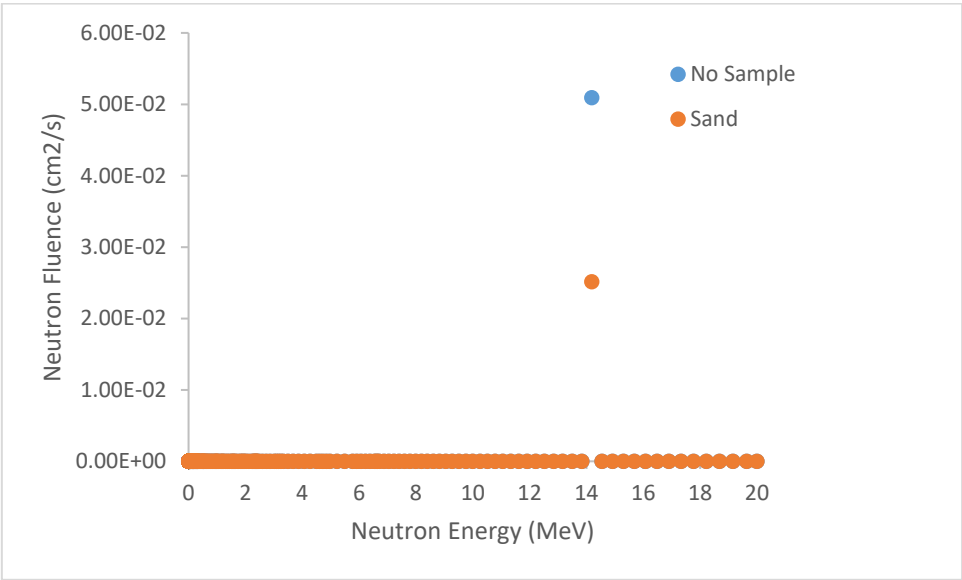

Figure 6.4 Neutron fluence as a function of energy of a 14 MeV neutron incident on sand target

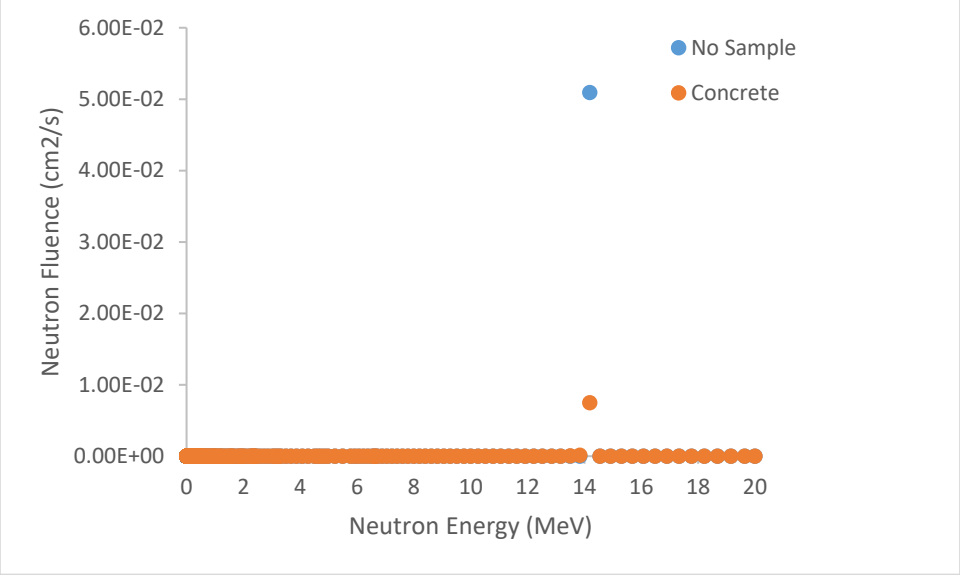

Figure 6.5 Neutron fluence as a function of energy of a 14 MeV neutron incident on concrete target

The neutron yields simulated with different concrete ingredients show similar general behaviour at the energy peak of about 14 MeV. All samples produces a more intense high-energy peak in the fast neutron energy region. These are neutrons which have not interacted. The spectra are calculated considering a USRTRACK detector in FLUKA, over a sensitive volume of 98.174 cm^3 as calculated in section 5.3.1. Neutrons are being detected as they are scattered in the target containing different shielding material respectively. The results shows that significantly more neutrons are being absorbed by the target as detected by the USRTRACK detector at 14 MeV energy region.

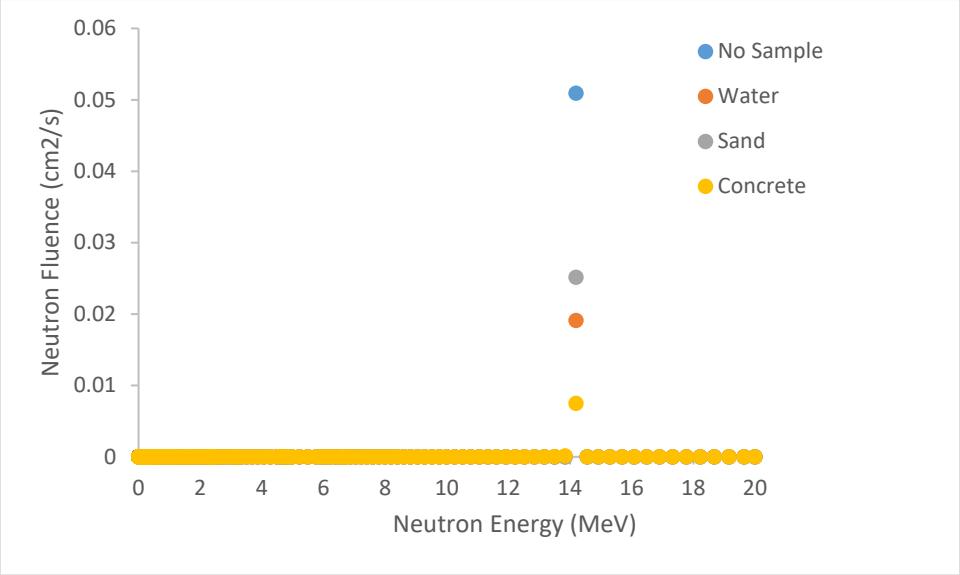

Figure 6.6 Total neutron fluence as a function of energy 14 MeV incident on all samples

Figure 6.6 depicts the fluence of all samples combined i.e. concrete and its ingredients. All samples have energies peaking at 14 MeV the rest of the fluence is close to zero. These simulations are highly simplified and do not include a container for any of the samples, or the surrounding environment, resulting in a clean 14.1 MeV contribution to the energy spectrum and very few scattered neutrons at lower energies. The differences between the simulation and experimental geometries are accounted for in the respective definitions of $I_0(E)$.

6.3 Comparison of Experiments with Simulations

In this section, the results of the study are presented and discussed with reference to the objective of the study, which was to to calculate the neutron distribution in the nuclear materials found in nuclear facilities that are used for shielding, and to develop corresponding simulation models and compare them with experimental results to validate the reliability of the software coding.

At the nuclear physics laboratory at the University of Cape Town (UCT), experiments are being conducted to measure the shielding capacity of concrete and other nuclear materials. Figures 6.7 through 6.10 shows the comparison of neutron transmission factor ($I(E)/I_0(E)$) as a function of the thickness (t, cm) of shielding material such as water, sand, cement and concrete, respectively. For the case of water, sand and cement measurements were made in increments of 1.0 cm, up to 10.0 cm, in increments of 1.0 cm. The concrete samples were made in several

thicknesses providing a range of 3.2 cm to 20.0 cm. The transmission curves showed an exponential decrease as a function of the shielding thickness which may be represented by the relation in equation 2.6. In the analysis, the exponential equation was then converted to a linear equation by taking the logarithmic on both sides of the equation then plot ln ($I(E)/I_0(E)$) v/s thickness (t) of the material.

The results of any two experiments can only be meaningfully compared if the intervals associated with each of the results are known.

More specifically:

- If the intervals that represent the results of two measurements overlap, then we say these two results "**agree within experimental uncertainty**."
- If the intervals that represent the results of two measurements do not overlap, then we say these results "**do not agree within experimental uncertainty**."

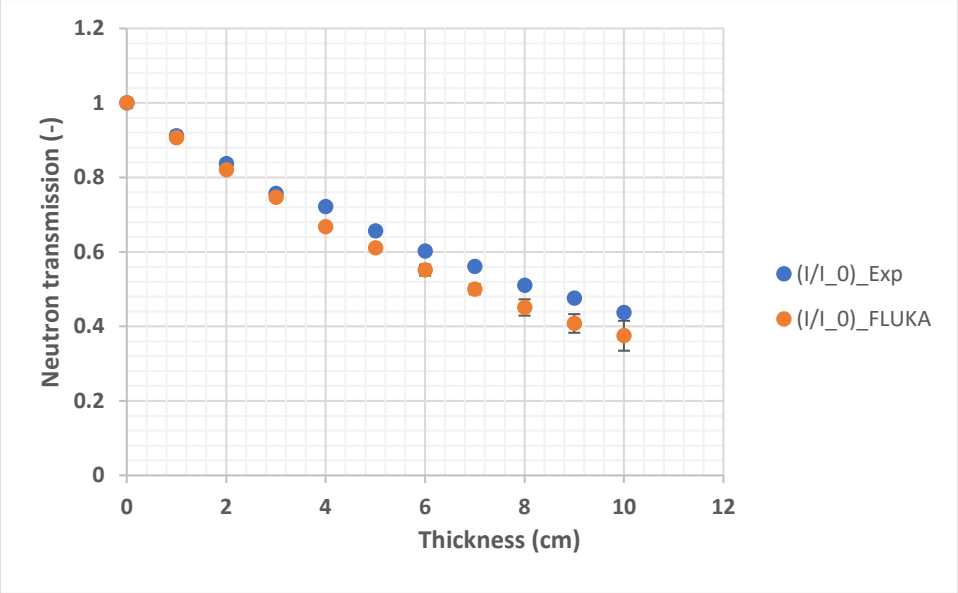

Figure 6.7 Neutron transmission factor ($I(E)/I_0(E)$) vs shielding thickness for water

In this graph the vertical error bars show the intervals of the neutron transmission values. It can be seen on the graph in figure 6.7 that the intervals of the values are overlapping, i.e. for water, the results for the experiments and FLUKA simulation agree within experimental uncertainty. The points agree with each other at around 68% confidence limit (i.e. within one standard deviation). The agreement between experimental results and studies on neutron

transport with FLUKA confirms that water is a good moderator of fast neutrons and that FLUKA can be used as an alternative way to experiment for this kind of studies. Furthermore, this suggests that water can also be used for shielding of neutrons at various energies.

Figure 6.8 depicts the results obtained from FLUKA as well as the experimental results, of 14 MeV neutron shielding by sand for a thickness of 10 cm. It can be seen from the graph in Figure 6.8 that the intervals of the values are overlapping, i.e. the simulation results of the neutron shielding obtained from FLUKA are in satisfactory agreement with the experimental results within experimental uncertainty. This agreement is quantified by having a very small deviations with overlapping intervals of results as seen on the graph. These small deviations may have occurred as a result of specification of material properties in the target during the simulation/experiment. Similar to water as a target, the agreement between experimental results and studies on neutron transport with FLUKA simulations confirms that sand is good shielding material of fast neutrons, and that FLUKA can be used as an alternative way to experiment for this kind of studies. This also suggests that sand can also be used for shielding of neutrons at various energies.

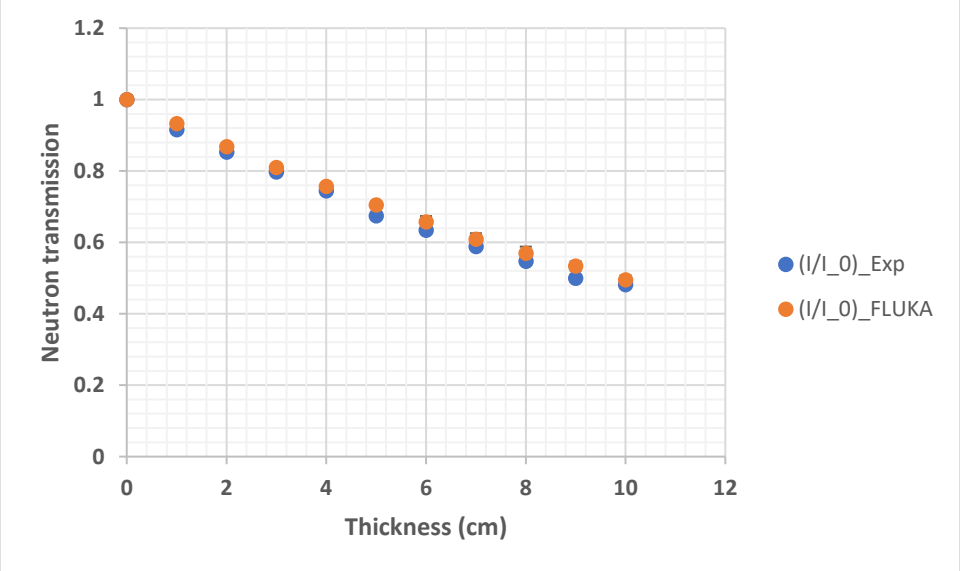

Figure 6.8 Neutron transmission factor ($I(E)/I_0(E)$) vs shielding thickness for sand

Figure 6.9 shows the simulation and experimental results for cement as a shielding material. In the case of cement, the simulation results of the neutron transmission obtained from FLUKA are in satisfactory agreement with the experimental results within experimental uncertainty. This agreement is quantified by having a very small deviations as seen on the graph. Similar to water and sand, the agreement between experimental results and studies on neutron transport with FLUKA simulations confirms that cement is a good shielding material of fast neutrons, and that FLUKA can be used as an alternative way to experiment for this kind of studies. This also suggests that cement can also be used for shielding of neutrons at various energies.

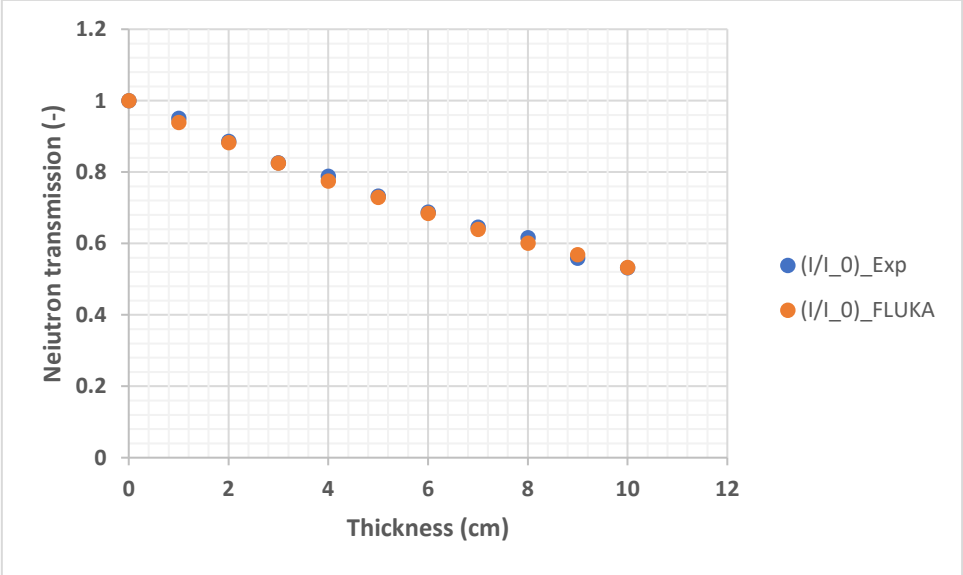

Figure 6.9 Neutron transmission factor ($I(E)/I_0(E)$) vs shielding thickness for cement

Figure 6.10 depicts the simulation and experimental results for concrete as a shielding material. In the case of concrete, the results for both approaches show different graphs at specific values of material thickness, i.e. some of the values are apart from each other but the intervals are overlapping. Therefore, the two graphs are in exact agreement with each other, with some minor deviations, i.e. they agree within experimental uncertainty. The observed general differences between the experimental and FLUKA values could be attributed to the various sources of experimental errors, such as material specifications in the input, in both experimental and simulation. On the other hand, this difference may be resolved by revising either both simulations and experiments or one of them. It is necessary to verify that all

elements in the input for the simulation are the same as those of the experiment to identify the main course of the discrepancy in the results.

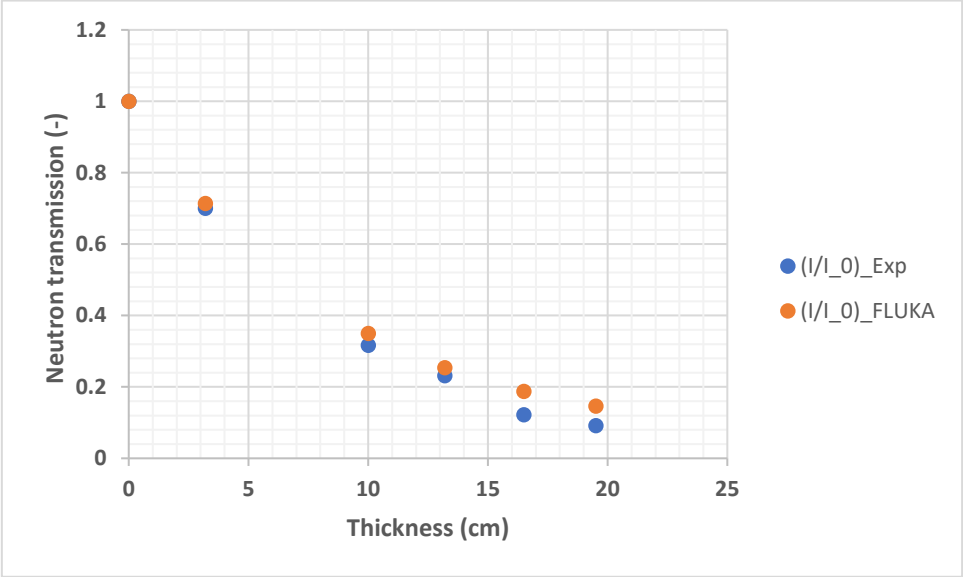

Figure 6.10 Neutron transmission factor ($I(E)/I_0(E)$) vs shielding thickness for concrete

There was a missing experimental data set between 5 -10 cm of material thickness, and also the measurements were taken at thicknesses greater than 10 cm i.e. different from other materials. As a result the simulations were then performed at exactly the same points for comparison and validation as seen in the graph on figure 6.11.

Summary

From the comparisons given above, the results are summarized as follows:

- There are no major differences between FLUKA and experimental measurements,
- The comparison generally agrees for water, sand, cement and concrete,
- Minor deviations were obtained on all target material (water, sand, and cement), which may suggest a need to be revised either experiment/simulation,
- These minor deviations may have originated from the specifications of the material compositions in the inputs and or other sources of errors within experiment/simulation

6.4 Removal cross-section ($\sum_R$)

The values of the removal cross-section for all samples were determined using weighted linear least squares fit method that was described in section 2.2.4. This was done through applying equations 2.8 through to 2.12 to the experiments and simulation data in Excel for all samples. The obtained results are shown in table 6.1 and they show general agreement between the FLUKA and Experiments.

Table 6.1 Removal cross-section for concrete ingredients for 14 MeV neutrons

	Density (g/cm^3)	$\sum_R(cm^{-1})$	
		Experiments	**FLUKA**
Water	1.00	0.08183 +/- 0.00042	0.09914 +/- 0.00022
Sand	1.46	0.07425 +/- 0.00040	0.07017 +/- 0.00019
Cement	1.38	0.06354 +/- 0.00045	0.06319 +/- 0.00017
Concrete	2.30	0.12298 +/- 0.00022	0.10378 +/- 0.00054

The uncertainties are statistical only, but there may be other sources of uncertainty (systematics, models, nuclear data, etc.) that are not accounted for here.

Figure 6.12 depicts the comparison of the removal cross-sections for all samples analysed. There is a good agreement between experiments and simulation for both sand and cement respectively. There is about 0.02 cm^{-1} difference in the value of the removal cross-section in the experiments and simulations for both water and concrete respectively. The experimental data presented for water deviate from the expected behavior above 4.0 cm, suggesting that there was a change in experimental conditions. It is recommend that this measurement is

repeated in the future. In the case of concrete, there were many air bubbles present in the sample which were not simulated and may have affected the calculated removal cross section. We recommend that several repeat measurements are made in the future to reduce the effect of non-uniformities in the sample.

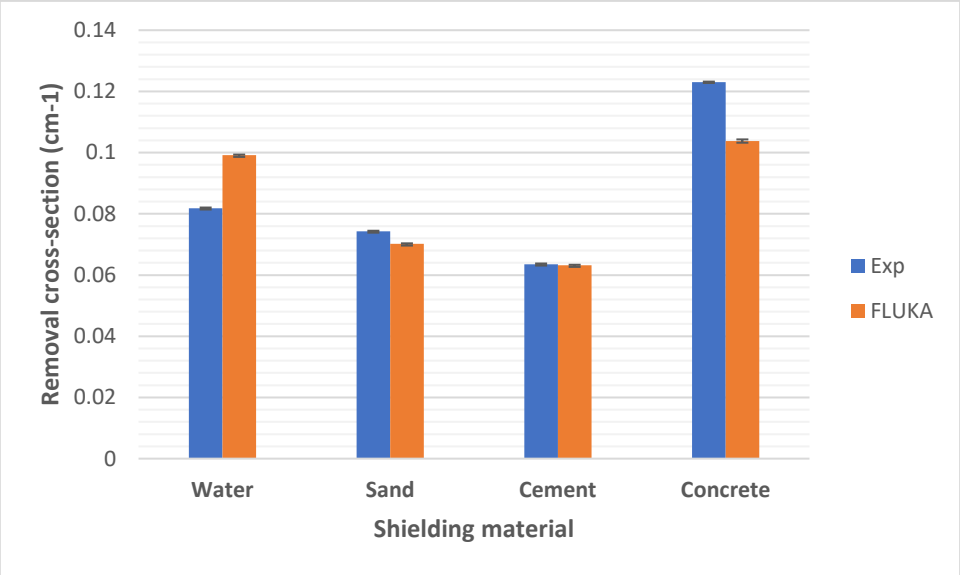

Figure 6.11 Removal cross-section

7 CONCLUSION

In this study, different concrete ingredients which are widely used as nuclear materials were evaluated for their neutron shielding performances utilizing experiments and simulations using FLUKA. The experimental setup of the neutron shielding by concrete at the UCT's nuclear physics laboratory, n-lab, was replicated in FLUKA. The objective of this work was to perform validation by running FLUKA simulations against experimental set up and also to investigate the neutron fluence through concrete target from neutrons originated from a collimated point source. In this section, the conclusion on FLUKA simulations and their reliability is discussed.

The aim of this validation project was not only to compare the results obtained in different shielding materials, but also to determine reliability of results from FLUKA in simulating the shielding capability of concrete. In this chapter, the results of testing the hypothesis that was stated in Chapter 1 are presented. The hypothesis states that the use of the Monte Carlo method in radiation transport is an effective way to predict the experimental results of the interaction of radiation with matter. The Monte Carlo method provides a better understanding of neutron transport through nuclear shielding materials and it can also be used to explain the relationship between theory, experiments and simulations in radiation transport.

7.1 Conclusion and Remarks

The effective removal cross section of concrete was measured by simulation to be 0.1038 +/- 0.0005 cm^{-1} and by experiment to be 0.1230 +/- 0.0002 cm^{-1} for the 14 MeV energy, illustrating broad agreement, and the complexity of simulating real composite materials such as concrete.

Experimental data for the simulated geometry set-up, produced good results, which implies that FLUKA was setup and used correctly. FLUKA simulations are able to reproduce experimental data for transport with good results. However, the results were not exact match as there were some deviations. The deviations then suggests that the material properties and the preparation of the sample in the input needs to be verified, in either experiments or simulations or both. These findings indicate that FLUKA simulations can be a good choice in estimating the radiation shielding parameters of concrete.

It can be concluded from this work that the selection of a shielding material for fast neutron requires the knowledge of the macroscopic effective removal cross-section. The results

obtained from this study can be used as a database for designers of nuclear technology. It can also be concluded that the macroscopic effective removal cross-section for fast neutrons is dependent on chemical content and density of shielding materials.

The relative comparisons of $\sum_R$ values for the samples and standard concrete materials that have relatively fair fast-neutron shielding behaviour (FNSB), so the agreement between the simulated results and the experimental values is quite promising. Some uncertainties about actual geometry, preparing the sample and material composition still exist. These uncertainties may also be explained by the fact that the simulation is in many ways "too perfect" in that the material is exactly the composition given for all of the material rather than having a more real distribution in content. The results of model validation could be used to improve or calibrate the model.

7.2 Limitations and Recommendations

Several improvements and additional experiments can be performed in order to further investigate the shielding properties of the materials. On the technicalities involved in this study, there aren't many recommendations on future work. However, based on the findings of this study, as a next step, it will be necessary to study the beam at different angles to the sample and compare the total energy fluence at each angle.

The following key recommendations are made:

a) Develop user skills by providing necessary training prior to applying knowledge on the project;
b) Apply an iteration process between simulations and experiments to identify one or more major causes and effect they have on the geometry and verify these major causes one by one to resolve the observed discrepancies;
c) Employ/Benchmark against one or more Monte Carlo codes (MCNP) to determine the source of error from one of the two methods;
d) Thoroughly review and verify that all materials and design features are correctly specified;
e) Develop a database to record, analyse, and examine the discrepancies observed in all methods to identify the source of error and allow for more accurate predictions, simulation and experiments;

REFERENCES

Agostinelli, S. et al., 2003. Geant4—a simulation toolkit. In: *Nuclear Instruments and Methods in Physics Research.* s.l.:Elsevier Science, p. 250–303.

Andrews, J., 2010. *Using FLUKA to Study Radiation Fields in ERL Components,* Washington: University of Washington.

Bastürk, M., Kardjilov, N., Lehmann, E. & Zawisky, M., 2005. *Monte Carlo Simulation of Neutron Transmission of Boron-Alloyed Steel,* s.l.: IEEE Transactions on Nuclear Science.

Bergstrom, I., 2013. *Minimizing the background radiation in the new neutron time-of-flight facility at CERN. FLUKA Monte Carlo simulations for the optimization of the n TOF second experimental line,* Lulea University of Technology, Sweden: Dep. of Engineering Sciences and Mathematics.

Böhlen, T. et al., 2014. *The FLUKA Code: Developments and Challenges for High Energy andMedical Applications,* s.l.: Nuclear Data Sheets 120.

Buffler, A. & Hutton, T., 2020. *Characterization by fast neutrons of concrete for nuclear facilities,* Cape town: Metrological and Applied Sciences University Research Unit, University of Cape Town.

Buffler, A., Hutton, T. & Leadbeater, T., 2019. Neutron transmission studies for concrete used in the nuclear industry. *International Journal of Modern Physics: Conference Series.*

Chan, Y. F., 2012. *Neutron Activation Measurements for Materials Used in Fusion Reactors,* Heslington: Department of Physics University of York.

Cho, N. & Chang, J., 2009. *Some Outstanding Problems in Neutron Transport Computation,* Daejeon, Korea: Korea Atomic Energy Research Institute.

El Abd, A., Mesbah, G. & Mohammed, N. M., 2017. A simple Method for Determining the Effective Removal Cross Section for Fast Neutrons. *Journal of Radiation and Nuclear Applications,* pp. 53-58.

Elmahroug, Y., Tellili, B. & Souga, C., 2013. *Calculation of fast neutron removal cross-sections for different shielding materials,* s.l.: s.n.

Engdahl, S., 2015. Validation of Ion Therapy Dose Calculation Algorithms by Monte Carlo.

Ferrari, A., Sala, P., Fasso`, A. & Ranft, J., 2005. *FLUKA: a multi-particle transport code,* s.l.: CERN-2005-10 .

Ferrari, A., Sala, P. & Ranft, J., 2018. *FLUKA Manual: Fluka: a multi-particle transport code.* GENEVA: CERN.

Ganapol, B., 2008. *Analytical Benchmarks for Nuclear Engineering Applications Case Studies in Neutron Transport Theory,* s.l.: Department of Aerospace and Mechanical Engineering University of Arizona.

Greenwald, M., 2004. Beyond Benchmarking: How Experiments and Simulations Can Work Together in Plasma Physics. *Computer Physics Communications,* p. 1–8.

Hack, E. et al., 2018. *Steps towards Industrial Validation Experiments.* Brussels, Belgium, MDPI.

Hutton, T. & Buffler, A., 2017. A new D-T neutron facility at UCT. *Proceedings of SAIP2017*.

Kleijnen, J., Ridder, A. & Rubinstein, R., 2010. *Variance Reduction Techniques in Monte Carlo,* s.l.: Tolburg University.

Mohammed, M. et al., 2016. Evaluation of variance reduction techniques in BEAMnrc Monte Carlo simulation to improve the computing efficiency. *Journal of Radiation Research and Applied Sciences,* pp. 424 - 430.

Mokhov, N. & James, C., 2017. *The MARS Code System User's Guide,* Illinois: Fermi National Accelerator Laboratory.

Mostafa, A. et al., 2020. *Multi-objective optimization strategies for radiation shielding performance of BZBB glasses using Bi2O3: A FLUKA Monte Carlo code calculations,* s.l.: Materials Research and Technology.

Msutwana, S., Buffler, A. & Hutton, T., 2019. *BSc (Honours) Thesis - Effective Removal Cross-section Based on Fast Neutron Energy Spectrum Analysis,* Cape town: University of Cape Town.

Oberkampf, W. & Trucano, T., 2007. *Verification and Validation Benchmarks,* s.l.: Nuclear Engineering and Design.

Pelowitz, D., 2011. *MCNPX user's manual – version 2.7.0,* USA.: Los Alamos National Laboratories.

Rata, R., Lee, S. & Barlow, R., 2016. FLUKA Simulations for Radiation Protection at 3 Different Facilities. *Proceedings of IPAC2016,.*

Sahadath, M., Biswas, R., Huq, M. & Mollah, A. S., 2017. *Calculation of the Neutron Shielding Properties of Locally Developed Ilmenite-Magnetite (I-M) Concrete,* Dhaka, Bangladesh: s.n.

Sargent, R., 2011. *Verification and Validation of Simulation Models.* Syracuse, NY 13244, U.S.A., Winter Simulation Conference.

Sariyer, D., Kucer, R. & Kucer, N., 2015. Neutron Shielding Properties of Concretes Containing Boron Carbide and Ferro – Boron. *Procedia - Social and Behavioral Sciences,* p. 1752 – 1756.

Sato, T., Niita, K., Matsuda, N. & Hashimoto, S., 2013.. Particle and Heavy Ion Transport code System, PHITS, version 2.52. *Nuclear Science and Technology,* Volume Vol. 50, No. 9,, p. 913–923.

Sharma, A., Sayyed, M. I., Agar, O. & Tekin, H., 2019. Simulation of shielding parameters for TeO2-WO3-GeO2 glasses using FLUKA. *Results in Physics.*

Shukla, D., 2015. Reactor Criticality Computations in Neutron Transport Theory Using Monte Carlo Method.

Shultis, J. & Faw, R., 2010. Radiation Shielding and Radiological Protection. In: *Handbook of Nuclear Engineering,.* USA: Department ofMechanical and Nuclear Engineering, Kansas, pp. 1316 - 1442.

Tekin, H., Altunsoy, E. & Kavazd, E., 2019. Photon and neutron shielding performance of boron phosphate glasses for diagnostic radiology facilities. *Results in Physics,* pp. 1457-1465.

Tekin, H., Singh, V. P., Manici, T. & Altunsoy, E. E., 2017. Validation of MCNPX with Experimental Results of Mass Attenuation Coefficients for Cement, Gypsum and Mixture. *Radiation Protection and Research 2017;42(3),* pp. 154-157.

Trucano, W., Oberkampf, L. & Timothy, G., 2007. *Verification and Validation Benchmarks,* United States of America: Sandia National Laboratories.

Uğur, F. A., 2017. *New Applications and Developments in the Neutron Shielding,* s.l.: EPJ Web of Conferences.

Vaz, P., 2009. *Neutron transport simulation (selectedtopics),* Portugal: Elsevier Ltd.

Vlachoudis, V., 2009. Flair: A Powerful But User Friendly Graphical Interface. *New York: American Nuclear Society.*

Wu, Y., 2017. Chapter 2: Neutron Transport Theory and Simulation. In: *Fusion Neutronics.* Singapore : Springer Nature , pp. 21-64.

APPENDIX: The FLUKA Input Cards

As stated by Bergstrom (2013), the minimum requirements for a FLUKA simulation is to define the beam, the geometry, the materials (unless only using the FLUKA material library) and the requested scoring (the MC estimators). The FLUKA input file is a plain text file containing the full description of the particle beam, geometry, materials, physics and scoring as well as the number of primary particles (histories) and executables needed to run a FLUKA simulation. The output files are usually binary and special subroutines are needed to read the outputs and to process and analyze the data. The FLUKA input file is structured as follows:

1. Beam definition
2. Geometry description
3. Material properties
4. Scoring definition (choice of estimators)
5. Initialization of random number
6. START the simulation
7. STOP the simulation

A.1 Building the input file in FLAIR

The input file is composed of command lines (so called input cards) which is the set of lines describing one command or property (e.g. beam specification or a geometry body). In FLAIR the input cards are interpreted as small blocks (or dialogues) for each FLUKA card providing the user with the possible options and with numerical fields when required.

In this section some of these cards, which have been used in the FLUKA simulations presented in this dissertation, are described in more details.

1. General information

General project information like title, notes, override formatting options for the input file.

2. Beam definition

All cards describing the source and the primary particles. With the BEAM card a beam is defined by its particle type, momentum or energy and the distribution.

With the BEAMPOSition card the position and direction of the beam is defined and in the START card sets the number of primary particles (= number of histories) used in the MC simulation.

3. Geometry

The FLUKA code is based on an optimized version of the Combinatorial Geometry package. The geometry must be specified by bodies (either solid bodies or half-infinite regions of space) and the physical regions determined by these bodies. Each BODY card describes the type, size and location of the body.

Regions are part of the geometry with a uniform material composition. They are defined by Boolean operations (addition, subtraction or intersection) of the defined bodies. A REGION card can consist of more than one Boolean expression (so called zones or sub-regions) but the zones does not necessarily have to be continuous. The complete geometry needs to be encapsulated by an external region defined by a solid body, usually a sphere or a box. This external region is assigned black hole (see Materials below) in order to stop the tracking of particles (because the ray tracing routines in FLUKA cannot track across the outermost boundary). In the simulation set-up, the region was defined according to the geometry set-up described in section 5.2 following the Boolean operation.

4. Media

This category includes the MATERIAL, COMPOUND and ASSIGNMAt cards, all describing the composition of materials and properties of the regions. Every region has to be assigned a material (with the ASSIGNMAterial card) including vacuum (no absorbance) and black hole (infinite absorbance). The black hole is a fictive material with infinite absorption used to terminate particle trajectories. A material is either pre-defined in FLUKA or user-defined. The materials can be simple elements (specific isotopes can be specified if the corresponding cross-section exists in the libraries) or compounds (compound, mixture or alloy). All materials needs the atomic number, the atomic weight and density. For compounds the chemical composition is given in atomic, mass or volume fractions, where the elements needs to be previously defined materials, but the density of the compound has to be given explicitly.

5. Scoring definition

With the scoring cards the user defines what quantities are of interest (i.e. the MC estimators) and instructs FLUKA which output files should be created. In the scoring definition the output files are configured by choosing the physical quantities of interest and how they should be estimated.

The output file from each scoring is chosen in formatted (ASCII) or unformatted (binary) units specifying the unit number. Several scorings can be combined in the same output file by scoring them in the same unit. All the binary output files can be post-processed, merged and graphically visualized in FLAIR.

6. Initialization of random number

Following these configurations is the random number initialization and the FLUKA simulations starts with a requested number of histories (primary particles) and ends when the stop command has been reached.

7. START the simulation

The number of primaries for all simulations can be selected to start the simulation.

8. STOP the simulation

Lastly the input file contained the STOP card to terminate the simulation.

A.2 Running the Simulation

With the Run Frame the user has the ability to run the simulation or create several runs by overriding some parameters. Each run is identified by a unique input name and is based on the same input file. The parameters that can be changed are the title of the run, random number seed, starting particles, and to activate or deactivate preprocessor define cards. To increase the statistics or to benefit of a multi-core or cluster architecture, the user can submit many runs based on the same input by changing the random number history (Vlachoudis, 2009). FLAIR is monitoring the progress on the run by inspecting the information on the files

created by FLUKA, rather than using the process information. FLAIR performs a series of complicated tests based on the time elapsed, the information that is written by FLUKA.

A.3 Inspecting the Files

FLAIR contains a file explorer that lists the files generated by FLUKA, grouped per FLUKA run, cycle and special ones like temporary files during the run. This frame gives the possibility to the user to inspect the output files even during the run and also to perform a clean up of the directory without losing the important files.

A.4 Data processing

To assist the user, FLAIR automatically detects all output files generated by FLUKA and their type from the input file definition and creates automatic rules for post processing these data. The user, simply by pressing a button starts the process and the data from all cycles are "merged" using the standard FLUKA post-processing routines. These rules can be fully customized by the user if required.

A.5 Plot Generation

FLAIR offers the possibility to the user to visualize in a graphical way the output of FLUKA. Currently with FLAIR one can plot the following (Vlachoudis, 2009):

- Geometry: 2D cross sections of the geometry either as boundary lines or color plots superimposed with materials, regions, lattices or magnetic field maps;
- Single differential quantities: through a common interface all single differential tallies like track length estimators, boundary crossing, collision or yield estimators. FLAIR allows to super impose many data on the same plot and even external files like experimental data for comparison;
- Double differential quantities: represented as a surface or color plots from estimators like boundary crossing or residual nuclei information;
- 3D mesh data: as two dimensional cross sections of 3D binning data, superimposed with the geometry, or as projection on a single axis;

- 3D photo realistic: the geometry can be exported to a ray tracer format, and photo realistic images can be generated with the use of Povray;

All plotted information could be normalized either by a fixed value or a user defined expression of the result. FLAIR is providing an interface to the user to define the desired plotting parameters which are sent to gnuplot to perform the actual plot. There are several text widgets for every plot frame that allow the user to send commands directly to the plotting program in order to allow to exploit the full power of gnuplot. To assist the user FLAIR provides also an automatic tool that scans the input file and proposes default plots for every scored quantity.